Finite-Rate Control: Stability and Performance

by

Sridevi Vedula Sarma

Submitted to the Department of Electrical Engineering and Computer Science
in partial fulfillment of the requirements for the degreeof Doctor of Philosophy

at the

MASSACHUSETTS INSTITUTE OF TECHNOLOGY

February 2006

Author .....
Department of Electrical Engineering and Computer Science
February 2, 2006

Certified by .....
Munther A. Dahleh
Full Professor
Thesis Supervisor

Accepted by .....
Arthur C. Smith
Chairman, Department Committee on Graduate Students

Finite-Rate Control: Stability and Performance

by

Sridevi Vedula Sarma

Submitted to the Department of Electrical Engineering and Computer Science
on February 2, 2006, in partial fulfillment of the
requirements for the degree of
Doctor of Philosophy

Abstract

The classical control paradigm addressed problems where communication between one plant and one controller is essentially perfect, and both have either discrete or continuous dynamics. Today, new problems in control over networks are emerging. A complex network involves an interconnection of numerous computational components where the controllers may be decentralized, and the components can have discrete or continuous dynamics. Communication links can be very noisy, induce delays, and have finite-rate constraints. Applications include remote navigation systems over the internet (eg. telesurgery) or in constrained environments (eg. deep sea/Mars exploration). These complexities demand that control be integrated with the protocols of communication to ensure stability and performance.

Control over networks is recent and continues to receive growing interest. Initial work has focused on asymptotic stability under finite-rate feedback control, where the only excitation to the system is an unknown (but bounded) finite-dimensional initial condition vector. Such problems reduce to state-estimation under finite-rate constraints. More recently, disturbance rejection limitations were derived for the same setting, assuming stochastic exogenous signals entering the system. Although these studies have contributed greatly to our understanding of such systems, input-output stability, performance analysis, and synthesis of coding schemes and controllers under finite-rate constraints remains largely untapped. In this thesis we address how finite-rate control impacts input-output stability and performance, and we also construct computable methods for synthesizing controllers and coding schemes to meet control objectives.

We first investigate how finite-rate feedback limits input-output stability and closed-loop performance. We assume that exogenous inputs belong to rich deterministic classes of signals, and perform analyses in a worst case setting. Since our results are derived using a robust control perspective, we are able to translate performance demands into optimization problems that can be solved to obtain quantization strategies and controllers in a streamlined manner. We then study how finite-rate feedforward control impacts finite-horizon tracking and navigation. We derive performance limitations for each case, and illustrate time and performance tradeoffs.

Finally, we investigate feedforward control over noisy discrete channels, and solve a decentralized distributed design problem involving the simultaneous synthesis of a block coding strategy and a single-input single-output linear time-invariant controller. We also illustrate delay versus accuracy tradeoffs.

Thesis Supervisor: Munther A. Dahleh
Title: Full Professor

To Rahil...

Love Mama

Acknowledgments

Over the last 10 years, I have enjoyed interacting with family, friends, colleagues, and professors, many of whom played a critical role in my graduation coming to a successful completion.

First, I'd like to thank my colleagues in my research group. I received much appreciated advice and encouragement from my seniors, including Fadi, Soosan, Nuno, Costas, Nicola, Ulf, Jorge, and Reza. I also enjoyed discussions with other colleagues, including Keith, Danielle, and Georgios. Finally, I am happy to see the positive energy brought in by new students, Mike, Erin, Holly, and of course Sleiman.

Second, I'd like to mention some friends who have supported me on many fronts. Ola, also a colleague whom I enjoyed learning Topology and playing squash with, often went above and beyond to help me through some difficult trials and tribulations. Jen, Surekha, Kamilah, and recently Jess, have also been there for me, and have always delivered in providing a much needed outlet with our daily-diary emails and "girls-night-out" gatherings. I value their honesty and appropriately-timed dishonesty! Finally, I thank two childhood friends, Iilun and Paulina, for sticking with me all these years and for providing unconditional support and love like sisters do.

Third, I cannot leave MIT without acknowledging some professors who made a real difference in my academic and life decisions. Prof. Bertsekas played a vital role in my move from SLS to LIDS, and has continued to encourage my studies. Prof. Massaquoi inspired me with his work and dedication and showed me exciting problems in neuroengineering. Prof. S. Salapaka, provided valuable discussions and continues to support me in academia. Prof. Shamma is an inspiration to me. He is incredibly creative and generous and I look forward to working with him in my future. I also appreciate Prof. Mitter, Prof. Megretski, and Prof. Feron for serving on my thesis committee and for providing fruitful discussions. My interactions with Prof. Megretski were extremely educational as he demands precision and clarity, which proved valuable to successfully solving seemingly difficult problems. Finally, I'd like to thank Prof. Dahleh for accepting me as his student and believing in me,

even when I doubted myself. Not only did I have the amazing opportunity to benefit from his tutelage and advice, I also built a company with him and had the privilege of being his coworker. As his coworker, I gained even more respect for his exceptional brilliance, sincerity, patience, restraint, diplomacy, integrity, and his generosity.

Finally, I thank my family. My extreme gratitude first extends to my father, Vedula Sarma. He supported my education and activities throughout my childhood and throughout my graduate studies. Because my father is a man of few words, my mother, Krishnaveni, complimented his support with intense affection and love. Her daily phone calls, although not always answered, have always been greatly appreciated. Aruna, my sister, continues to be an amazing role model, with two wonderful (and crazy) kids and a splendid academic career in her pocket. Rajan, my husband and my confidant, has been there for me from the beginning. He is an exceptional student, researcher, consultant, and not to mention tennis and squash player, and he continues to show me how to succeed. I am honored to be his wife, confidant, and mother of his child. His family has also been very supportive of my education, and I am grateful to them. Finally, I thank my son Rahil. He has demanded structure to my schedule, which has made me incredibly productive over these past few months. He makes my stressful schedule bearable, and he lights up my world with his clinching hugs, beautiful smile, bright eyes, kind heart, and wonderful sense of humor. This thesis is dedicated to him.

Contents

List of Figures

List of Tables

Chapter 1

Introduction

1.1 Network Systems

In the early to mid-1900s, stability and performance of the classical control system were extensively studied. This classic loop consists of one plant and one centralized controller. The communication links between the plant and controller are either assumed to be perfect or have little noise, and the clocks in both the plant and controller are assumed to be synchronized. Finally, both plant and controller either have discrete dynamics or continuous dynamics.

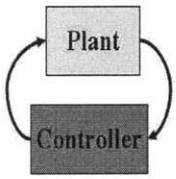

Figure 1-1: Classical Control System

In today's "information-rich world", computation, communication and sensing are cheaper and ubiquitous, and opportunities in control are exploding. We now face the problem of control in network systems. A typical network is much more complex than the classic control system. It may involve an interconnection of numerous computational components as opposed to just two. The controllers may be decentralized, and

the links can be very noisy, induce delays, and have finite-rate constraints. The clocks inside the computational components may not be synchronized, and the components can have either discrete or continuous dynamics. These complexities demand that control be integrated with the protocols of communication to ensure stability and performance. Thus, a revolution in this area would be to generate a unifying theory for communication, computing, and control.

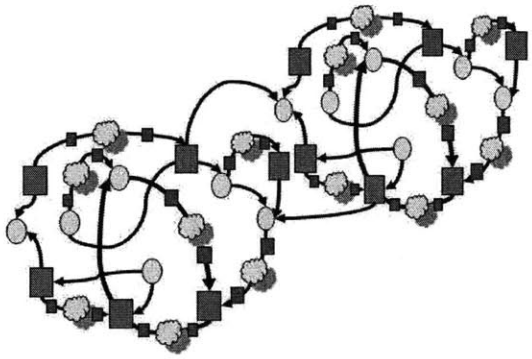

Figure 1-2: Network System

An example of such a complex system is a network in a future car (see Figure 1-3). Today, cars have multiple control systems that roughly can be classified as follows:

1. *Powertrain Control*: includes systems that basically are involved in powering the wheels (engine, transmission, differential, axles, etc)
2. *Multi-Media Control*: radio, DVD, GPS etc.
3. *Safety Control*: anti-lock breaks, traction control, stability control, airbags, seatbelts, etc.
4. *Emmisions Control*: fuel consumption
5. *Body Control*: windows, windshield wipers, automatic door locks, etc.

Today many or all of these systems communicate with each other, but in the near future, we anticipate that these systems will become much more complicated

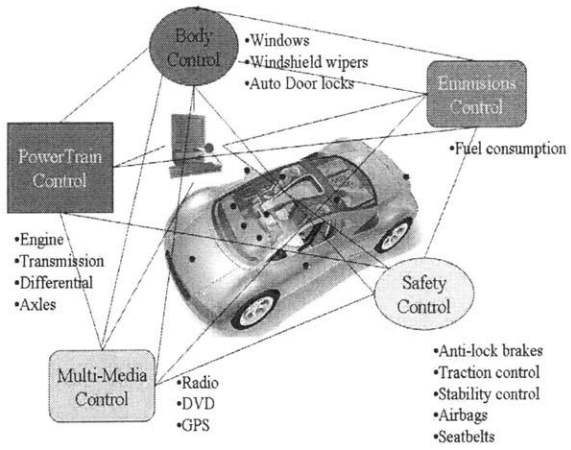

Figure 1-3: Network System in Future Car

and will require a network, *i.e.,* an interconnection of computers, to coordinate their functions within the car, and to coordinate information outside of the car. In the presence of such a network, stability, performance, and most importantly safety, are real concerns.

1.2 Two Simple Networks

In most complicated networks, a basic core loop can be extracted. This basic network consists of two computational components and two communication links (see Figure 1-4). A communication link is made up of three components, a channel encoder, channel, and channel decoder, which are briefly described below.

- *Channel (C)*: A channel is an operator that takes in a string of symbols and outputs a string of symbols. It's bandwidth is defined by its transmission rate, R_c, which indicates the number of symbols per second that the channel can transmit with each use. This corresponds to a delay of l/R_c seconds if the input string of symbols has length l. If the channel is assumed to have infinite

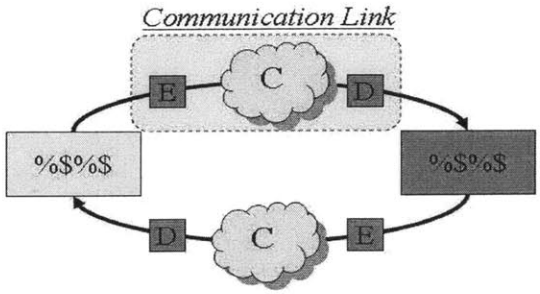

Figure 1-4: Basic Network Loop

bandwidth, then it can transmit any input with no delay. A channel may also corrupt its input by adding noise, which may either be independent of its input or dependent on its input. Typically, a communication channel is modeled probabilistically with a conditional distribution of producing an output sequence of symbols given an input sequence of symbols.

- *Channel Encoder & Decoder* (E, D): The channel encoder and decoder are operators designed to reduce the deleterious effects of the channel via a cooperative strategy. To minimize the effects of the noise added by the channel, the encoder may first pre-process its input. In addition, to adhere to the bandwidth limits of the channel, the encoder maps its input, which in general may require an infinite number of symbols to describe, to a finite set of symbols or codeword via some quantization scheme. The decoder typically knows the operations of the encoder and decodes appropriately. An example of a primitive coding

strategy is when the channel encoder makes copies of the codeword it produces from its input, and then sends these copies through an infinite-bandwidth noisy channel. The channel decoder then uses knowledge of this repetition to decode the link input via a majority-rule algorithm, *i.e.*, it guesses that the input is the symbol 'A' if it observed that 3 out of the 5 times that the input symbol was sent resulted in an 'A' at the decoder end. The disadvantage of such a primitive scheme is that sending copies of symbols over the channel results in more channel uses and hence more transmission delays.

From the basic core loop, we extract a simple feedback network and a simple feedforward network, as shown in Figure 1-5.

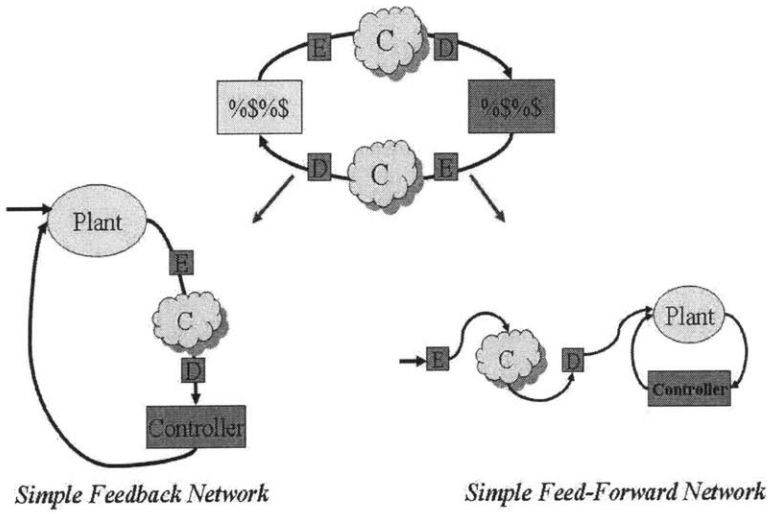

Figure 1-5: Basic Network and Two Simple Networks

In the feedback setting, the plant and feedback controller are separated by a communication link. Here, both stability and performance are impacted by the location of the communication link. A second link connecting the controller output to the plant

input is excluded in our set up for simplicity of analysis. In the feedforward setting, the plant and controller are both local to each other, and are driven by a remote reference command that must travel through a communication link before exciting the plant. Here, only performance is impacted by the location of the communication link. Much work has been done regarding these two simple networks, and some important results are discussed next.

1.3 Literature Review

In this section, we review previous studies that are most relevant to each of the two set ups that we consider in this thesis. In doing so, we highlight differences between our work and others.

1.3.1 Simple Feedback Network

The simple feedback network, shown in Figure 1-6, has been extensively studied over the past 10 years. Researchers have considered both stochastic and deterministic frameworks, a variety of stability notions, and different types channels in the communication link. Most studies, however, either consider the case in which no external inputs are applied to the control system, and derive conditions on the channel rate required for various notions of *asymptotic stability*, or allow exogenous inputs to be bounded, and derive conditions on the channel rate that guarantee that the system's state or output is bounded. In this thesis, we consider two deterministic classes of exogenous inputs, and focus on finite-gain stability (defined in section 1.3.1), which requires the plant output to scale with the input, as opposed to just being bounded. We restrict our attention to finite-rate noiseless channels, with rate R, in this review and in this thesis.

Another important difference between our work and most previous works, is the class of encoders we consider. To clearly distinguish between the encoder constructed in this thesis from those designed in previous investigations, we classify all encoders into 4 types of operators, defined by 2 features: *memory* and *control access*. The

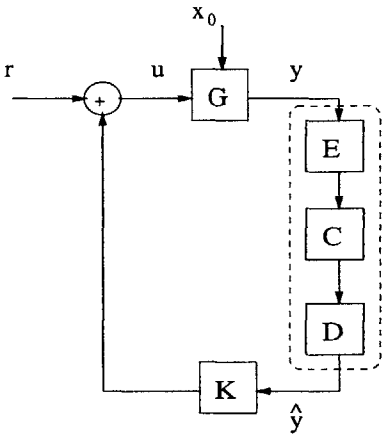

Figure 1-6: Simple Feedback Network

memory property divides all encoders into memoryless and not memoryless; and the control access property separates encoders that either have access to the plant input, u, or can compute u exactly, from those that have no knowledge of u. Being able to compute u assumes that the encoder knows the control law and has enough memory to compute what the controller, K, generates at any time t; and that there is no noise between the feedback signal and the reference command, r. In our work and in others, the encoder and decoder know bounds on the plant's initial condition, and on all exogenous signals described in the set up (reference or disturbance), and the plant dynamics. We discuss the 4 encoder classes below, and reference relevant work.

1. *Has Memory and Has Control Access*:

   When the encoder is either physically local to the plant or if the encoder knows the controller it must communicate with, then it can be modeled as belonging to this class. This class of encoders enables derivations of a necessary and sufficient conditions on the channel rate required to guarantee asymptotic stability and finite-gain input-output stability (defined and discussed in section 1.3.1). The well-known condition that guarantees both notions of stability, for G having state-space description $ss(A, B, C, 0)$, is $R > \sum_i max(0, log_2(|\lambda_i(A)|)$, where $\lambda_i(A)$ denotes the ith eigenvalue of A. Note that the rate condition is independent of the controller, K, which makes sense as the encoder and decoder both

have access to u ($r = 0$), and thus the controller's effects on the plant output can be subtracted off in both the encoder and decoder. Tatikonda's encoder class I from [29] is equivalent to this class. Other works that consider encoders from this class include [2, 22, 23, 25, 26, 31].

2. *Has Memory and Has No Control Access*:

   If the encoder is not local to the plant and if it does not know what controller will receive the signal it sends through the channel, then it can be modeled as belonging to this class. This class of encoders is considered in this thesis. We derive sufficient conditions for finite-gain stability as a function of the encoder and controller for a family of reference inputs (Theorem 2.2.1). Since there is no control access, the information describing the plant output, that must be conveyed through the channel, is characterized by an infinite number of parameters. Therefore errors due to the channel do not converge to zero, which makes deriving the minimal rate required for stability a difficult search over all possible encoders, decoders and controllers. This is discussed in more detail at the end of this section. We set out to achieve finite-gain stability, which relates y to r, since our ultimate objective is to obtain desired properties from the plant output y, given that r comes from some class of signals. Other works that consider encoders that fall into this class include [7, 8, 10, 13, 14], however all of these consider an initial condition exciting the system ($r = 0$), and study some notion of asymptotic stability or bounded state stability (eg. containability [8]). Some also allow the rate to be countable as opposed to finite [13].

3. *Memoryless and has Control Access*:

   This is identical to Tatikonda's encoder class II, and a sufficient condition for asymptotic stability, as a function of the plant and controller dynamics, is derived in [29]. For example, if G is first-order with state space description $ss(a, b, 1, 0)$, and the controller is a gain, $K = k$, then $R > \max(0, log(\frac{|bk}{1-|a+bk|}))$, is a sufficient condition to ensure asymptotic stability. Since the encoder is memoryless, it cannot send more and more information about any single parameter

describing the plant output, and therefore, errors due to the channel do not converge to zero. This makes deriving necessary conditions on the rate required for stability a search over all possible encoders, decoders and controllers, which again is difficult and not pursued in [29].

4. *Memoryless and has No Control Access*:

   To our knowledge, no one has considered this class of encoders, as these operators cannot do anything more than to allocate R bits to the input it receives at a given time step. A special case of the encoder constructed in this thesis falls into this class, and we derive sufficient conditions on the channel rate required to guarantee finite-gain stability in this case (Corollary 2.2.1).

Stability Results

We now put into perspective results for different notions of stability under finite-rate feedback for deterministic settings. Since most studies consider encoders that have memory and control access, we review results for this class only. Our hope is to not only review important results, but to differentiate our set up, which consider encoders that have memory but no control access, from the many prior investigations regarding such systems. First, we discuss asymptotic stability, and then consider finite-gain input-output stability when the initial condition on the plant's state is zero. We conclude our review with a theorem that states necessary and sufficient conditions on the channel rate to guarantee both notions of stability.

We consider the following model of the system shown in Figure 1-6.

$$\begin{aligned} x_{t+1} &= Ax_t + B(v_t + r_t) \quad \forall t \geq 0, \\ y_t &= Cx_t, \\ v_t &= K(\hat{y}_t), \end{aligned} \tag{1.1}$$

where $t \in \mathbf{Z}_+$, $x_t \in \mathbb{R}^n$, and $r_t, y_t, v_t \in \mathbb{R}$.

When possible, we present simple analyses and reference generalizations to avoid having technical details distract the reader from the objectives of this section.

- **Asymptotic Stability**: When only an initial condition excites the system, stability is defined with respect to an equilibrium point. A vector $x_0 \in \mathbb{R}^n$ is an *equilibrium point* of the system, if $\forall t \geq 0,\ x_t = x_0$. That is, if the system starts in an equilibrium, it stays there for all time. It is not difficult to see that system (1.1) only has one equilibrium point at the origin.

  The origin of a system is *asymptotically stable* (AS) if the following hold.

  1. Lyapunov Stability: For each $\epsilon > 0$, there exist a $\delta(\epsilon) > 0$ such that

  $$||x_0||_\infty < \delta(\epsilon) \Rightarrow ||x_t||_\infty < \epsilon,\ \forall t \geq 0.$$

  2. Attractivity: There is an $\eta > 0$, such that

  $$||x_0||_\infty < \eta, \Rightarrow x_t \to 0 \text{ as } t \to \infty.$$

  Lyapunov stability forces all trajectories to remain within ϵ-balls, when the initial state vector lies in δ-balls, where δ is a function of ϵ. Attractivity forces all trajectories near the origin to actually approach the origin as t grows. Note that trajectories can approach the origin in very strange ways, without staying within an ϵ-ball for all time. Thus, there exist systems for which the origin is attractive but not Lyapunov stable.

- **Finite-Gain (FG) Stability:** Assume now that the initial state vector $x_0 = 0$, while r is nonzero. Finite-gain stability requires the norm of the output to scale linearly with the norm of the input (as opposed to just being bounded). Formally, a system with input r and output y is *FG*-stable if there exists a finite positive constant α, and a finite constant β such that

$$||y||_\infty \leq \alpha||r||_\infty + \beta, \quad \forall r \ \ s.t \ \ ||r||_\infty \leq \overline{r}.$$

Note that if $\alpha = 0$, then we get bounded-imput implies bounded-output (BIBO) stability. It turns out that FG stability is impossible under finite-rate feedback for $\beta = 0$, and a general proof of this limitation for arbitrary memoryless channels and using an information theoretic viewpoint, can be found in [24]. As discussed in section 3.3, one of our control objectives is to design the controller to minimize β.

Theorem 1.3.1. *Consider encoders that have memory and control access. Assume* $||r||_\infty \leq \overline{r}$. *Then, system (1.1) is*

1. *asymptotically stable,*
2. *and FG stable*

if and only if $R > \sum_i max(0, log(|\lambda_i(A)|)$.

Proof.

Our proof here follows from those given in [29].

- *(Necessity): Assume that the state is the output of the system* ($C = I$), *and that the* A *matrix is diagonal with all eigenvalues being unstable. The general case is treated in [29]. Without loss of generality, we can assume that for a finite positive constant vector* $L \in \mathbb{R}^n, \Omega_0 = \{x \in \mathbb{R}^n : x \leq L\}$.

  1. *For a given control sequence* $\{u_0, u_1, ..., u_{t-1}\}$, *we know that* $x_t = A^t x_0 + \sum_{i=0}^{t-1} A^{t-1-i} B u_i$. *If the system is AS, then* $\forall \epsilon > 0$ *and* $\forall x_0 \in \Omega_0$, *there exists a* $T(\epsilon, L)$ *such that* $\forall t \geq T(\epsilon, L)$ *we have* $||x_t|| \leq \epsilon$. *In particular this holds for* $\epsilon < L$. *For this value of* ϵ, *define the sets* Γ, *parameterized by control sequences* $u_0^{t-1} \triangleq \{u_0, u_1, ..., u_{t-1}\}$, *to be*

$$\Gamma_{u_0^{t-1}} = \{x_0 \in \Omega_0 : ||x_t|| \leq \epsilon\}.$$

Note that x_t depends linearly on $u_0, u_1, ..., u_{t-1}$, hence all the Γ sets are linear translations of each other with the same volume, $|det(A^{-t})|K_d\epsilon^d$. A lower bound on the channel rate is then computed by counting how many Γ sets it takes to cover Ω_0 at time t.

$$\begin{aligned} R > & \quad \frac{1}{t} log \frac{vol(\Omega_0)}{vol(\Gamma)} \\ = & \quad \frac{1}{t} log \frac{K_d L^d}{|det(A^{-t})|K_d\epsilon^d} \\ = & \quad \sum_i max(0, log(|\lambda_i(A)|) + \frac{d}{t} log(\frac{L}{\epsilon}). \end{aligned}$$

Since $\epsilon < L$, the second term approaches 0, as $t \to \infty$.

2. *The set of points that x_t can take contains the following:*

$$\Omega_t = \{x | x = A^t x_0 + \sum_{i=0}^{t-1} A^{t-1-i} B r_i + \sum_{i=0}^{t-1} A^{t-1-i} B v_i, \quad \forall x_0 \in \Omega_0, ||r||_\infty \leq \overline{r}\}.$$

Let $\Omega_t^{zero} = \{x | x = A^t x_0 + \sum_{i=0}^{t-1} A^{t-1-i} B v_i, \quad \forall x_0 \in \Omega_0\}$, be the set of all points $x_t \in \Omega_t$ where r is set to zero. Suppose the system is FG-stable, then there exists an encoder and decoder such that the estimation error $e_t = x_t - \hat{x}_t$, is bounded, i.e., $||e_t||_\infty \leq \overline{e}$ (every signal in the loop is bounded, so x_t, $\hat{x}^t$, and their difference are all bounded). A lower bound on the rate can be computed by counting the number of regions of diameter less than $2\overline{e}$ it takes to cover Ω_t for any $t \geq 0$. Therefore, we require a rate of at least

$$\begin{aligned} R > & \quad \frac{1}{t} log \frac{vol(\Omega_t)}{K_d \overline{e}^d} \\ = & \quad \frac{1}{t} log \frac{vol(\Omega_t^{zero})}{K_d \overline{e}^d} \\ = & \quad \sum_i max(0, log(|\lambda_i(A)|) + \frac{d}{t} log(\frac{L}{\overline{e}}), \end{aligned}$$

where the second inequality follows from $\Omega_t^{zero} \in \Omega_t$, and the third inequality follows from our proof above for asymptotic stability. Note that $\frac{d}{t}log(\frac{L}{e})$ is bounded and becomes negligible as $t \to \infty$.

- *(Sufficiency): To prove sufficiency, we first fix the controller to be any stabilizing state-feedback controller, K, and choose the encoder to be a "primitive quantizer" as defined in [29]. At time t, this encoder receives x_t and outputs a channel symbol σ_t. For simplicity, we assume that $n = 1$, i.e., the plant G is first-order. The general case is shown in [29]. In the first-order case, the primitive quantizer has 2 states:*

  1. *c_t: centroid of quantizer support region at time t,*
  2. *L_t: defines the boundaries of quantizer support region at time t, i.e., $\{c_t - L_t, c_t + L_t\}$,*

  which have the following evolution equations for $t \geq 0$:

$$c_{t+1} = a\hat{x}_t + bu_t \quad c_0 = 0,$$
$$L_{t+1} = \frac{a}{2^R} L_t + b\overline{r} \quad L_0 = L.$$

  The state estimate is the output of the encoder, i.e., $\hat{x}_t = \sigma_t$. Figure 1-7 illustrates the support region of the quantizer at time t. The state x_t lands somewhere in the support region which is divided into 2^R partitions. The state then gets encoded into σ_t, which is the center of the the partition in which x_t lands. The decoder then uses σ_t, as the state estimate at time t, and sends this to the controller K. It is guaranteed that x_t lands somewhere in the support region for all $t \geq 0$, because x_0 automatically lands in the support region by definition of L_0, and the evolution of L_t captures the evolution of x_t. Specifically, the partition in which x_t lands will grow by a factor of (a) in one time step, but will then shrink by a factor of (2^R), to form new partitions at time $t + 1$.

  Assume that $R > log(a)$, then the following shows that the state-estimation error is bounded, where the bound is proportional to $\overline{r}$.

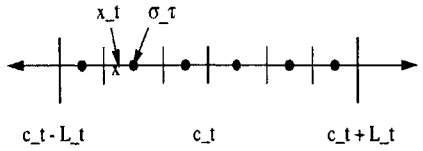

Figure 1-7: Quantizer Support Region defined by c_t and L_t.

$$
\begin{aligned}
|e_t| = |x_t - \hat{x}_t| = & \quad |\tfrac{L_t}{2^R}| \\
= & \quad 2^{-R}|(\tfrac{a}{2^R})^t L + \textstyle\sum_{i=0}^{t-1} a^{t-1-i} b\overline{r}| \\
\leq & \quad 2^{-R}\{|(\tfrac{a}{2^R})^t L| + |b|\overline{r}\textstyle\sum_{i=0}^{t-1}|a|^{t-1-i}\} \\
\rightarrow & \quad \tfrac{2^{-R}|b|\overline{r}}{1-|a|} \triangleq \overline{e}.
\end{aligned}
$$

Next, we show that x_t is bounded for all $t \geq 0$. To do so, we apply the certainty equivalent controller, and get that the control input at time t is $u_t = K\hat{x}_t + r_t$. Then, $x_{t+1} = (a+bk)x_t - bke_t + br_t$, which gives us the following.

$$
\begin{aligned}
|x_t| \quad & = |-\textstyle\sum_{i=0}^{t-1}(a+bk)^{t-1-i}bke_i + \sum_{i=0}^{t-1}(a+bk)^{t-1-i}br_i| \\
& \leq |\textstyle\sum_{i=0}^{t-1}(a+bk)^{t-1-i}bke_i| + |\sum_{i=0}^{t-1}(a+bk)^{t-1-i}br_i| \\
& \leq |bk|\overline{e}|\textstyle\sum_{i=0}^{t-1}(a+bk)^{t-1-i}| + |b|||r||_\infty \textstyle\sum_{i=0}^{t-1}|a+bk|^{t-1-i} \\
& \leq \tfrac{|bk|\overline{e}}{|a+bk|-1}(|a+bk|^t - 1) + \tfrac{|b|||r||_\infty}{|a+bk|-1}(|a+bk|^t - 1) \\
& \rightarrow \tfrac{|b|(|k|\overline{e}+||r||_\infty)}{1-|a+bk|}.
\end{aligned}
$$

Thus, the system is asymptotically stable ($||r||_\infty = \overline{r} = 0 \rightarrow$, $|x_t| \rightarrow 0$), and FG stable.

■

There are some important comments to make at this point. If the encoder did not have access to the control input, then the primitive quantizer state evolution equation for the centroid c_t cannot involve u_t exactly. Rather, it would have to involve some known bound on the control input. In addition, if the encoder did not have memory, the notion of "states" disappears, and the quantization support region cannot, in general, shrink over time. The ability to derive necessary and sufficient conditions for stability, regardless of which type, becomes more complicated.

In chapter 2, we show that FG stability is also possible for encoders that have memory but no control access, and derives sufficient conditions on the required channel rate. The encoder constructed to prove sufficiency belongs to a parameterized family of time-varying quantizers, which is defined and discussed in more detail in section 2.1.1.

Control Access vs. No Control Access

When encoders have access to the control signal or can compute the control signal exactly, the plant output signal that must be communicated down to the decoder, can be described by a finite number of parameters. More concretely, $y_t = CA^t x_0 + C\sum_{i=0}^{t-1} A^{t-1-i}Bu_i$. Therefore, the only quantity unknown to E and D is x_0, which is just a vector of n numbers that belong to a bounded set in $\mathbb{R}^n$. Therefore, assuming G is observable, the encoder can compute x_0 after n time steps and start transmitting x_0 through the channel down to the decoder, at a rate of R bits per time step. Consider an encoder that allocates R_i bits to the ith component of x_0, such that $\sum_i R_i = R$, while the decoder continues to update its approximation of x_0 and x_t. The error vector then evolves as follows:

$$e_t = x_t - \hat{x}_t = A^t(x_0 - \hat{x}_{0,t}),$$

where $\hat{x}_{0,t}$ is the estimate of x_0 at time t. If we assume that A is diagonal, [1] we get the following upper bound on the magnitude of each error component:

[1] All results hold for general A matrices as shown in [29].

$$|e_t(i)| \leq L\{\frac{|\lambda_i(A)|}{2^{R_i}}\}^t \quad i = 1, 2, ..., n,$$

where $|x_0(i)| \leq L$, for $i = 1, 2, ..., n$. It is easy to see that if $R_i > max(0, log(|\lambda_i(A)|)$, for $i = 1, ..., n$, which implies that $R > \sum_i max(0, log(|\lambda_i(A)|)$, then the system is AS, since K is assumed to be stabilizing.

On the other hand, when the encoder does not have access to any signal in the loop except for the plant output, the unknown quantities characterizing y_t are x_0 and $u_0, u_1, u_2...$, which are an infinite number of parameters. From the encoder and decoder's perspective, the output of the plant is suddenly very "rich." For any fixed t, the decoder must approximate $y_0, y_1, ..., y_t$. These approximations cannot converge to their actual values, and the best strategy that E and D can employ is to improve the approximations over time by allowing E to allocate more and more bits to them (this motivates our construction of the quantizer presented in section 2.1.1). The system boils down to a quantized feedback system, which is difficult to analyze, and where the usual tradeoff of delay versus accuracy holds.

1.3.2 Simple Feedforward Network

In the simple feedforward network (Figure 1-8), the plant and controller are local to each other, but are together driven by a remote reference signal that is transmitted through a communication channel. In this set up, the longer one spends coding the input signal before it enters the channel, the more accurate the signal is that drives the remote control system. However, delays in receiving commands at the remote site negatively affect performance. Since there is no outer feedback loop, only performance is affected by the location of the communication channel.

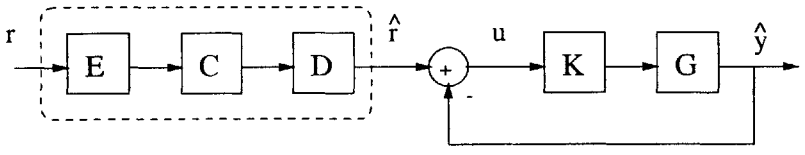

Figure 1-8: Simple Feed-Forward Network

There is much work that focuses on the reconstruction of the reference command at the remote site (see [34] and references therein). However, here we are interested in *navigating* a remote system with the reconstructed command. Most teleoperation systems, which often involve hazardous and unstructured tasks, can be addressed under this framework. Examples of such tasks include nuclear reactors, space applications, medical operations, and deep-sea and MARS explorations [21]. Such systems typically incorporate feedback as shown in Figure 1-9, and stability is impacted by the location of the communication channel.

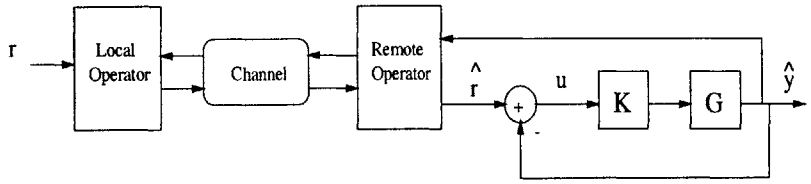

Figure 1-9: Remote Navigation with Feedback

Previous work involving communication constraints in remote navigation systems mainly consider noiseless channels that simply add delays. When the delays are assumed to be constant, then the local and remote operators compute wave-variable transformations [27] and/or are delay compensators [1], which transform the channel into a passive connection, thereby ensuring stability under any delay.

$$\int_0^t \dot{x} F d\tau \geq 0. \tag{1.2}$$

Note that the transformation of variables is such that

$$u = \frac{b\dot{x} + F}{2\sqrt{b}}, \quad v = \frac{b\dot{x} - F}{2\sqrt{b}}, \tag{1.3}$$

where b is an arbitrary positive constant. This enables the passivity condition in

equation (1) to be rewritten in terms of the magnitudes of the *wave variables* u and v as

$$\int_0^t (|u|^2 - |v|^2)d\tau \geq 0 \tag{1.4}$$

for all $t \geq 0$. Now consider the teleoperation system shown in Figure 1-10, consisting of a 2-port communication link connected to an arbitrary slave system. The communication link has an input vector $\dot{\mathbf{x}} = (\dot{x}_m, -\dot{x}_s)^T$ and output vector $\mathbf{F} = (F_m, F_s)^T$, and is passive if for all $t \geq 0$

$$\int_0^t \dot{\mathbf{x}}^{\mathbf{T}}\mathbf{F}d\tau = \int_0^t (\dot{x}_m F_m - \dot{x}_s F_s)d\tau \geq 0. \tag{1.5}$$

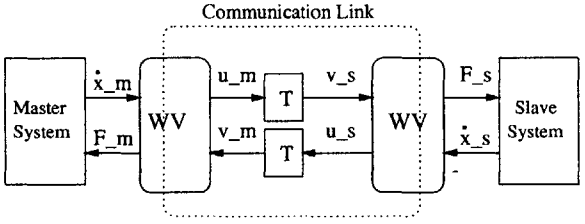

Figure 1-10: Wave Variable Teleoperation System

If in particular, the communication link consists of two wave variable (WV) transformers cascaded via a pure delay T, as shown in Figure 1-10, then condition (4) can be rewritten in terms of only the wave variables u_m and u_s (note that $v_s = u_m(t-T)$ and $v_m = u_s(t-T)$) as follows

$\int_0^t (\dot{x}_m F_m - \dot{x}_s F_s)d\tau = \left[\int_0^t u_m^2 d\tau - \int_0^t u_s^2(t-T)d\tau\right] - \left[(\int_0^t u_m^2(t-T)d\tau - \int_0^t u_s^2 d\tau.\right] \geq$
0.

The inequality can be reduced to

$$\int_{t-T}^t (|u_m|^2 + |u_s|^2)d\tau \geq 0,$$

which holds for all $t \geq 0$ irrespective of the delay T. In this case the communication link is always passive. It is easily shown that if the link is connected to a slave system via a negative feedback configuration as in Figure 1, the overall system, when viewed as a 1-port system with input $\dot{x}_m$ and output F_m (*i.e.*, from the master), is also passive if the slave is passive [27].

Although wave-variables account for stability under any delay, performance still degrades with delays. One design augments the wave-variable method with Smith predictors to reduce tracking errors [17]. When the delays are assumed to be time-varying but bounded from above, then buffering techniques [19] can be applied. Finally, if the channel also erases some signals (eg. packet losses), then one can develop a model of the channel using second-order statistics [5], or build an observer at the remote operator to reconstruct the data stream at the channel output [20] to maintain stability and performance.

Our approach uses the local operator as a channel encoder, and the remote operator as a channel decoder (as defined in information theory [16]) to minimize errors between the actual and reconstructed command. Our work combines information theory and robust control tools. We ignore feedback to focus on performance issues as the communication channel only impacts performance in such a setting. We analyze performance of the simple feedforward network for finite horizon objectives, and also construct methods to simultaneously design a controller, encoder and decoder to meet a specific infinite-horizon performance objective.

Chapter 2

Finite-Rate Feedback Control: Stability

In this chapter, we consider a system in which the plant and feedback controller are separated by a noiseless finite-rate communication channel. Previous work derive conditions on the channel rate that guarantee some notion of asymptotic stability when the system is excited by an initial condition, and when the encoder has memory, and more importantly, either has access to the control input or can compute it perfectly. These types of encoders enable derivations of necessary and sufficient conditions that are independent of the controller. Here, we allow for two deterministic classes of reference inputs to excite the system, and derive sufficient conditions for finite-gain stability as a function of the encoding strategy and controller. We consider a scenario in which the encoder does not have access to (and cannot compute) any signal in the system except for the plant output.

2.1 Problem Formulation

Consider the system shown in Figure 2-1, with the following dynamics.

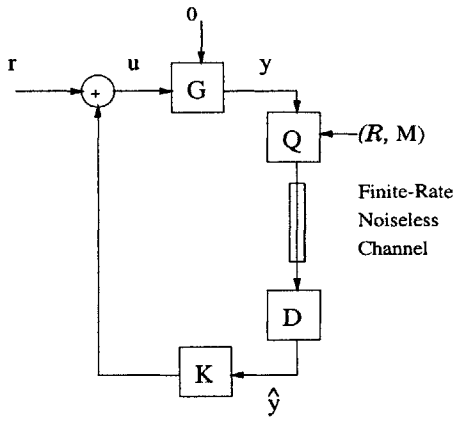

Figure 2-1: Simple Feedback Network

$$
\begin{aligned}
x_{t+1} = Ax_t + B(v_t + r_t) \quad \forall t \geq 0, \\
y_t = Cx_t, \\
v_t = K(\hat{y}_t),
\end{aligned}
\tag{2.1}
$$

where $t \in \mathbf{Z}_+$, $x_t \in \mathbb{R}^n$, and $r_t, y_t, v_t \in \mathbb{R}$. E is a limited-rate $(\mathcal{R}, M)$-quantizer, $E = Q(\mathcal{R}, M)$, which has *infinite memory*, and is *time-varying* in that the strategy it follows in allocating a total of R bits to all of the inputs up to time t, is a function of t (see section 2.1.1 for details). We assume that the channel can transmit R bits instantaneously with each use. The channel decoder, D, receives more information on the current and past values of y and sends these updates to the controller. Finally, K is a causal discrete-time time-varying linear system. Our goal is to ultimately design E, D and K to maintain finite-gain stability and to achieve multiple control objectives, such as tracking reference commands.

We define the closed-loop system to be FG-stable if for all $r \in \mathcal{C}_r$, there exists a finite positive constant α and a finite constant β such that $||y||_\infty \leq \alpha||r||_\infty + \beta$. Here, we investigate FG stability for a bounded class of reference inputs, $\mathcal{C}_r = l_{\infty,\bar{r}}$, where $l_{\infty,\bar{r}}$ is the class of all signals r such that $||r||_\infty \leq \bar{r}$.

2.1.1 Limited-Rate Time-Varying $(\mathcal{R}, M)$-Quantizers

Before stating the problems that we are interested in solving, we first define and model the parameterized class of time-varying infinite-memory $(\mathcal{R}, M)$-quantizers.

We view the quantizer as a module that approximates its input, which in general requires an infinite number of bits, with a finite number of bits. Formally speaking, an $(\mathcal{R}, M)$-quantizer with bit-rate R, is a sequence of causal time-varying operators, parameterized by an infinite-dimensional *rate matrix*, $\mathcal{R}$, which, in general looks like

$$\begin{bmatrix} R_{00} & 0 & 0 & \dots & \dots \\ R_{01} & R_{11} & 0 & 0 & \dots \\ R_{02} & R_{12} & R_{22} & 0 & \dots \\ \vdots & \vdots & \vdots & \ddots & \ddots \end{bmatrix},$$

such that $1 + \sum_j R_{ij} = R \ \ \forall i$, and an infinite-dimensional positive-definite diagonal *scale matrix*, $M = diag(M_{00}, M_{11}, M_{22}, ...,)$. The $(\mathcal{R}, M)$-quantizer saturates to output M_{kk}, the $(k+1)^{th}$ diagonal of M, when its input, y_k, has magnitude greater than or equal to M_{kk}, *i.e.*, when $|y_k| \geq M_{kk}$. However, we denote the quantizer "valid" only when $|y_k| \leq M_{kk}$ for all $k \geq 0$, and define what the quantizer does in this case below.

Let $\hat{y}_i(j)$ be the quantized estimate of y_i at time j. Then, $\mathcal{R}$ determines that at time $t = 0$, 1 bit is used to denote the sign of y_0, and R_{00} bits are used to quantize the magnitude of y_0 to produce $\hat{y}_0(0)$. At time $t = 1$, an *additional* R_{01} bits are used to quantize the magnitude of y_0 to produce $\hat{y}_0(1)$; 1 bit is used to denote the sign of y_1, and R_{11} bits are used to quantize the magnitude of y_1 to produce $\hat{y}_1(1)$, and so on. The accuracy of $\hat{y}_i(j)$ is within $\pm M_{ii} 2^{-\sum_{k=i}^{j} R_{ik}}$ of y_i for all $i \geq 0$.

More concretely, at any time t, the quantizer, channel, and decoder can be broken down into the five steps shown in Figure 2-2 when $|y_k| \leq M_{kk}$ for $0 \leq k \leq t$. First, the ith component of the vector y^t is scaled by $\frac{1}{M_{ii}}$ for $i = 1, 2..., t$, to produce z^t, where $y^t = [\ y_0 \ \ y_1 \ \ \dots \ \ y_t\ ]'$, and $M_t = diag(M_{00}, M_{11}, ..., M_{tt})$. The scaling by M_t^{-1} ensures that $||z^t||_\infty \leq 1$. Then, each element of z^t is converted into its binary representation, *i.e.*, a string of '0's and '1's in the Decimal-to-Binary (D2B) converter. Next, each

binary string is truncated according to the bit-allocation strategy induced by $\mathcal{R}$. Specifically, the binary string representing $z^t(i) = \frac{y_i}{M_{ii}}$ is truncated to contain only its first $(\sum_{j=i}^{t} R_{ij})$ bits. Note that this truncation induces an error of at most $2^{-\sum_{j=i}^{t} R_{ij}}$ in magnitude for $z^t(i)$, *i.e.*, $|z^t(i) - \hat{z}^t(i)| \leq 2^{-\sum_{j=i}^{t} R_{ij}}$.

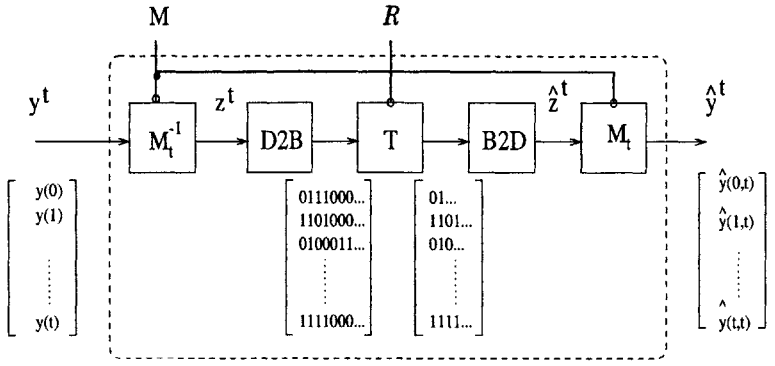

Figure 2-2: Quantizer-Channel-Decoder Operator at Time t

As shown in Figure 2-2, the truncated binary string is converted back into its decimal representation, via the Binary-to-Decimal module (B2D), to produce $\hat{z}^t$. Finally, $\hat{z}^t$ is scaled by M_t to produce $\hat{y}^t$, where $\hat{y}^t = [\ \hat{y}_0(t)\ \ \hat{y}_1(t)\ \ \hat{y}_2(t)\ \ \ldots\ \ \hat{y}_t(t)\ ]'$

An upper bound on the error between each input component and its approximate output is:

$$|y_k - \hat{y}_k(t)| \leq M_{kk} 2^{-\sum_{i=k}^{t} R_{ki}},$$

$\forall k \leq t$. Stated differently, if $|y_k| \leq M_{kk}$ for $0 \leq k \leq t$, then there exists a $w_k(t)$ with $sign(w_k(t)) = sign(y_k)$ and $|w_k(t)| \leq 1 \ \ \forall t \geq 0$, such that

$$\hat{y}_k(t) = y_k + M_{kk} 2^{(-\sum_{i=k}^{t} R_{ki})} w_k(t),$$

for all $k \leq t$.

For analysis, we augment the output of the quantizer at time t to be the vector of *all* estimates of $\mathbf{y}^t$ from time 0 to time t. We denote the augmented vector as $\hat{\mathbf{y}}_a^t$ as shown below.

$$\hat{\mathbf{y}}_a^t = \left[\begin{array}{c} \hat{y}_0(0) \\ \hline \hat{y}_0(1) \\ \hat{y}_1(1) \\ \hline \vdots \\ \hline \hat{y}_0(t) \\ \hat{y}_1(t) \\ \hat{y}_2(t) \\ \vdots \\ \hat{y}_t(t) \end{array}\right].$$

We can then model the quantizer in its "valid" region as the following sequence of time-varying operators:

$$Q(\mathcal{R}, M) = \{Q_t : \mathbb{R}^{t+1} \rightarrow \mathbb{R}^{\frac{(t+1)(t+2)}{2}} \mid Q_t(\mathbf{y}^t) = \hat{\mathbf{y}}_a^t = I_t \mathbf{y}^t + F_t(\mathcal{R})\overline{M}_t(M)\mathbf{w}_a^t, \quad t \geq 0\},$$

where

$$I_t = \left[\begin{array}{cc} 1 & \\ \hline 1 & 0 \\ 0 & 1 \\ \hline \vdots & \\ & \\ \hline & \\ I^{t\times t} & \end{array}\right],$$

and

$$F_t(\mathcal{R}) = \left[\begin{array}{c|c|c|c} f_{00} & & & \\ \hline & f_{01} & & \\ & & f_{11} & \\ \hline & & \ddots & \\ \hline & & & f_{0t} \\ & & & & \ddots \\ & & & & & f_{tt} \end{array}\right], \quad \overline{M}_t(M) = \left[\begin{array}{c|c|c|c} M_{00} & & & \\ \hline & M_{00} & & \\ & & M_{11} & \\ \hline & & \ddots & \\ \hline & & & M_{00} \\ & & & & \ddots \\ & & & & & M_{tt} \end{array}\right],$$

with $f_{ks} = 2^{-\sum_{i=k}^{s} R_{ki}}$ for $s = 0, 1, ..., t$, and $k = 0, 1, ..., s$.

Also,

$$\mathbf{w}_a^t = \left[\begin{array}{c} w_0(0) \\ \hline w_0(1) \\ w_1(1) \\ \hline \vdots \\ \hline w_0(t) \\ w_1(t) \\ w_2(t) \\ \vdots \\ w_t(t) \end{array}\right],$$

where $\mathbf{w}_a \in l_\infty$ such that $||\mathbf{w}_a||_\infty \leq 1$.

2.1.2 Plant and Controller

We represent the LTI causal system G and the causal linear time varying controller K as the following matrix multiplication operators at any time instance t:

$$G_t = \begin{bmatrix} g_0 & & & & \\ g_1 & g_0 & & & \\ g_2 & g_1 & g_0 & & \\ \vdots & & \ddots & \ddots & \\ g_t & \cdots & \cdots & g_1 & g_0 \end{bmatrix}, \quad K_t = \begin{bmatrix} k_0 & & & & & & \\ & k_1 & k_0 & & & & \\ & & & k_2 & k_1 & k_0 & \\ \vdots & & & & & & \ddots \end{bmatrix}.$$

We note that $K_t I_t = K_t^{LTI}$, where K^{LTI} is a LTI controller whose parameters, k_j for $j \geq 0$, characterize the time-varying controller K_t, and

$$K_t^{LTI} = \begin{bmatrix} k_0 & & & & \\ k_1 & k_0 & & & \\ k_2 & k_1 & k_0 & & \\ \vdots & & \ddots & \ddots & \\ k_t & \cdots & \cdots & k_1 & k_0 \end{bmatrix}.$$

If G and K^{LTI} are finite-dimensional, with state-space descriptions (A_g, B_g, C_g, D_g) and (A_k, B_k, C_k, D_k), respectively, then $g_0 = D_g$, $g_j = C_g A_g^{j-1} B_g$ for $j \geq 1$, and $k_0 = D_k$, and $k_j = C_k A_k^{j-1} B_k$ for $j \geq 1$.

Figure 2-3 illustrates the closed-loop system at time t when the quantizer is modeled as an endogenous disturbance as described in section 2.1.1, with

$$\mathbf{r}^t = \begin{bmatrix} r(0) \\ r(1) \\ \vdots \\ r(t) \end{bmatrix} \quad \& \quad \mathbf{u}^t = \begin{bmatrix} u(0) \\ u(1) \\ \vdots \\ u(t) \end{bmatrix}.$$

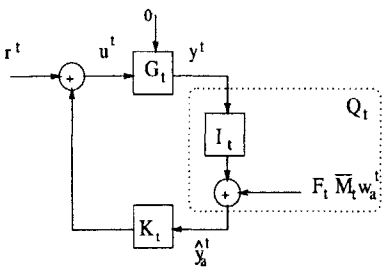

Figure 2-3: Control System at Time t

From here onwards, we refer to $F_t(\mathcal{R})$ as F_t and $\overline{M}_t(M) = \overline{M}_t$ for an easier read.

2.1.3 Problem Statement

We are interested in solving the following problems for each class of reference inputs, $\mathcal{C}_r$, defined earlier.

1. Given G, K, $\mathcal{C}_r$, and a rate matrix, $\mathcal{R}$, determine whether there exists a set of scale matrices, M, that maintain FG stability and quantizer validity.

2. Given G, K, and $\mathcal{C}_r$, characterize the set of all rate matrices, $\mathcal{R}$, such that the system is FG-stable and the quantizer is valid.

3. Within the set of stabilizing rate matrices, find the minimum transmission rate, R, of the channel.

2.2 Stability Analysis

In this section, we derive sufficient conditions for FG stability when $\mathcal{C}_r = l_{\infty,\bar{r}}$. Let $T_t \triangleq (I - G_t K_t^{LTI})^{-1} G_t$, then it is straightforward to show that $y^t = T_t r^t + T_t K_t F_t \overline{M}_t w_a^t$. The following theorem then gives sufficient conditions for FG stability and quantizer validity [1]. Note that for a matrix A, $\|A\|_1 = \max_i \sum_j |a_{ij}|$.

[1] One can add an exogenous input, d, at the input of the controller and derive sufficient conditions for external stability by computing transfer functions from r and d to y and v (output of the controller). We omit the details here as the analysis is straightforward.

Theorem 2.2.1. *Consider system (1) with $x_0 = 0$. Let $E = Q(\mathcal{R}, M)$, for a given rate matrix $\mathcal{R}$, and let $r \in l_{\infty,\bar{r}}$. If*

1. $||T||_1 < \infty$,
2. $||TKF||_1 < 1$,

then there exists a constant scale matrix $M = mI$, such that

- *(FG stability)* $||y||_\infty \leq ||T||_1||r||_\infty + m||TKF||_1$,
- *(quantizer validity)* $||y||_\infty \leq m$.

Proof. *Choose $m \geq \frac{||T||_1\bar{r}}{1-||TKF||_1} \geq 0$, which is possible given the norm bounds on r, T, and TKF. Then,*

$$\begin{aligned} ||y^t||_\infty = & \quad \sup_t\{||T_t r^t + T_t K_t F_t \overline{M}_t w^t||_\infty\} \\ \leq & \quad \sup_t ||T_t||_1||r^t||_\infty + \sup_t ||T_t K_t F_t \overline{M}_t||_1 \\ \leq & \quad ||T||_1||r||_\infty + m||TKF||_1 \\ \leq & \quad m. \end{aligned}$$

The last inequality comes from our choice of m.

■

The stability condition in Theorem 2.2.1 is *sufficient* as we have not yet proven that $|y_k| > m$, for any $k \geq 0$, renders the system unstable. Proving necessity is more difficult using this class of encoders, as it entails searching over all possible encoders, decoders and controllers, to find the triple that minimizes the rate required for FG stability.

We note that memoryless, time-invariant quantizers are represented by an identity rate matrix multiplied by the value of the fixed rate $R-1$, which leads to the following corollary.

Corollary 2.2.1. *Consider system (1) with $x_0 = 0$. Let $E = Q(\mathcal{R}, M)$, for a diagonal rate matrix $\mathcal{R} = (R-1)I$, and let $r \in l_{\infty,\bar{r}}$. If*

1. $||T||_1 < \infty$,
2. $||TK^{LTI}||_1 < 2^{R-1}$,

then there exists a constant scale matrix $M = mI$ such that

- *(FG stability)* $||y||_\infty \leq ||T||_1||r||_\infty + m2^{(1-R)}||TK^{LTI}||_1$,
- *(quantizer validity)* $||y||_\infty \leq m$.

Chapter 3

Finite-Rate Feedback Control: Performance

In this chapter, we show how our construction of the quantizer leads to the result that the set of allocation strategies that maintains stability for each class of reference signals is convex, allowing the search for the most efficient strategy to ensure stability to be formulated as a convex optimization problem. We then synthesize optimal bit-allocation strategies for a class of finite-memory quantizers for various plant and controller pairs, and observe that strategies that minimize the rate required for stability do not reduce to trivial memoryless bit-allocation strategies. Finally, we show how our framework enables synthesis of controllers to achieve multiple performance objectives under finite-rate feedback.

3.1 Characterization of Stable Rate Matrices

In chapter 2, we showed that if $||TKF||_1 < 1$, then the system is FG-stable for bounded reference inputs. This inequality can be written as a set *convex* constraints on the rate matrix parameters. The following theorem shows this result.

Theorem 3.1.1. *Let* $X = \{vec(\mathcal{R})\}$ [1] $= [\ R_{00}\ \ R_{01}\ \ R_{02}\ \ \ldots\ \ R_{11}\ \ R_{12}\ \ \ldots\ ]'$, *then*

[1] *The "vec" operator on a matrix simply concatenates all the column to form one large column vector.*

for any infinite dimensional matrix, P, the condition $||PF(X)||_1 < \eta$ is convex in X for any $\eta > 0$.

Proof.

$$||PF(X)||_1 < \eta \Leftrightarrow \sum_{j=0}^{\infty} f_j(X)|P_{ij}| < \eta \quad i = 0, 1, ...$$

where $f_j(X) = 2^{-\sum_{i=j}^{\infty} R_{ji}}$. We now show that $f_j(X)$ is convex in X, and thus any non-negative combination of $f_j(X)$ is convex. First, we recall that 2^{-a} is a convex function of a. Let $2^{-\sum_{i=j}^{\infty} R_{ji}} = 2^{-c_j' X}$, where c_j' is a row vector for $j = 0, 1, ...$

$$\begin{aligned} 2^{-\lambda(c_j' X_1)-(1-\lambda)(c_j' X_2)} &= 2^{-\lambda a_1-(1-\lambda)a_2} \\ &\leq \lambda 2^{-a_1} + (1-\lambda)2^{-a_2} \\ &= \lambda 2^{-c_j' X_1} + (1-\lambda)2^{-c_j' X_2}. \end{aligned}$$

■

If we let $P = TK$, then we get that the stability condition, $||TKF||_1 < 1$, is a set of convex constraints on the infinite dimensional vector $vec(\mathcal{R})$. This result enables the search for the most efficient quantizer to be formulated as a convex optimization problem. We solve for efficient bit-allocation strategies for finite-memory quantizers in section 3.2.

3.2 Synthesis of Bit-Allocation Strategies

In this section, we synthesize rate matrices for a class of finite-memory quantizers that minimize the channel rate required for FG stability.

3.2.1 Finite-Memory $(\mathcal{R}, M)$-Quantizers

We introduce a special class of practical quantizers that have finite memory and are periodic. Specifically, each value of y gets approximated by the quantizer for *at most*

N consecutive time steps. In fact, for any $t \geq 0$, y_{tN+j} gets approximated for $N-j$ time steps, for $j = 0, 1, ..., N-1$. Moreover, the bit-allocation strategy repeats every N time steps. We call this class of quantizers, "repeated-block" (RB) quantizers because the structure of the rate matrix is block diagonal as shown below.

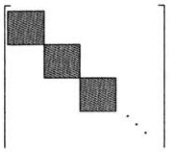

Each block is the following $N \times N$ matrix:

$$R_{block} = \begin{bmatrix} R_{00} & & & \\ R_{01} & R_{11} & & \\ \vdots & \vdots & \ddots & \\ R_{0,N-1} & R_{1,N-1} & \cdots & R_{N-1,N-1} \end{bmatrix}.$$

RB quantizers are time-invariant operators in "lifted" coordinates, where each time step in the lifted coordinates is equivalent to N time steps in original coordinates. We define the following lifted signals for $t \geq 0$:

$$\tilde{\mathbf{r}}_t = \begin{bmatrix} r_{tN} \\ r_{tN+1} \\ \vdots \\ r_{(t+1)N-1} \end{bmatrix}, \quad \tilde{y}_t = \begin{bmatrix} y_{tN} \\ y_{tN+1} \\ \vdots \\ y_{(t+1)N-1} \end{bmatrix},$$

$$\tilde{\mathbf{w}}_t = \begin{bmatrix} w_{tN}((t+1)N-1) \\ w_{tN+1}((t+1)N-1) \\ \vdots \\ w_{(t+1)N-1}((t+1)N-1) \end{bmatrix}.$$

The model for a repeated-block quantizer, Q_{RB}, in the lifted coordinates, denoted $\tilde{Q}_{RB}$, is:

$$Q_{RB}(\mathcal{R}, M) = \{\tilde{Q}_{RB} : \mathbb{R}^N \to \mathbb{R}^N \mid \tilde{Q}_{RB}(\tilde{y}) = \tilde{\hat{y}} = \tilde{y} + m\tilde{F}_N\tilde{w}\},$$

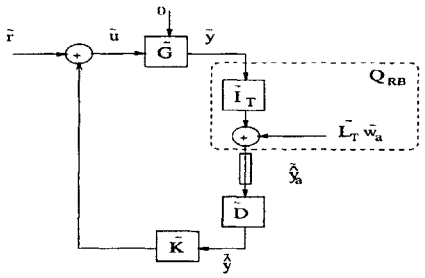

Figure 3-1: Lifted Closed-Loop System

where, written as a matrix multiplication operator, $\tilde{F}_N = diag(F_{N-1}, F_{N-1}, ...)$.

The closed-loop system in lifted coordinates is shown in Figure 3-1.

The system and controller in Figure 3-1 are defined as follows:

$$\tilde{G} = \begin{bmatrix} \tilde{g}_0 & & \\ \tilde{g}_1 & \tilde{g}_0 & \\ \tilde{g}_2 & \tilde{g}_1 & \tilde{g}_0 \\ \vdots & & \ddots \end{bmatrix},$$

where

$$\tilde{g}_0 = \begin{bmatrix} g_0 & & & \\ g_1 & g_0 & & \\ \vdots & & \ddots & \\ g_{(N-1)} & \cdots & & g_0 \end{bmatrix},$$

and for $j \geq 1$,

$$\tilde{g}_j = \begin{bmatrix} g_{jN} & g_{jN-1} & \cdots & g_{(j-1)N+1} \\ g_{jN+1} & g_{jN} & \cdots & g_{(j-1)N+2} \\ \vdots & & \ddots & \vdots \\ g_{(j+1)N-1} & \cdots & & g_{jN} \end{bmatrix},$$

$\tilde{K}$ is defined similarly and is an LTI controller in lifted coordinates!

We are now ready to state sufficient conditions for FG stability in the lifted coordinate space, but first state the following Lemma whose proof is straightforward and left to the reader.

Lemma 3.2.1. *Let P be any causal LTI SISO system, and $\tilde{P}$ is a lifted version of P with lift factor N. Then, for any $N \geq 1$, $||\tilde{P}||_1 \geq ||P||_1$.*

Theorem 3.2.1. *Consider system (1) lifted by a factor of N, with $x_0 = 0$. Let $E = Q_{RB}(\mathcal{R}, M)$, for a given repeated-block rate matrix $\mathcal{R}$, and let $r \in l_{\infty,\bar{r}}$. If*

1. $||(I - \tilde{G}\tilde{K})^{-1}\tilde{G}||_1 < \infty$, *and*
2. $||(I - \tilde{G}\tilde{K})^{-1}\tilde{G}\tilde{K}\tilde{F}_N||_1 < 1$,

then the system is FG-stable.

Proof. *If condition (1) and (2) hold, then by invoking Lemma 3.2.1, we get that $||(I - GK)^{-1}G||_1 < \infty$, and $||(I - GK)^{-1}GKF||_1 < 1$. From Theorem 2.2.1, we then get that the original system (un-lifted) is FG stable, which implies that the lifted system is FG stable.* ■

3.2.2 Examples

To find the minimum channel rate required for FG stability and the corresponding bit-allocation strategy, for a given plant and stabilizing controller, we solve the following convex optimization problem,

$$\begin{aligned} & & minR & \\ s.t.\ \ R = 1 + \sum_j R_{ij} & \quad i = 0, 2, .., N-1, & & (3.1) \\ ||(I - \tilde{G}\tilde{K})^{-1}\tilde{G}\tilde{K}\tilde{F}_N||_1 < 1, & & & (3.2) \\ R_{ij} \geq 0 & \quad j \leq i = 0, 2, .., N-1, & & (3.3) \end{aligned}$$

which is readily computable for the class of finite-memory quantizers with $N \times N$ repeated-block rate matrices.

For a given G and K, we lift the system by a factor of N, and denote the state-space description of $(I - \tilde{G}\tilde{K})^{-1}\tilde{G}\tilde{K}$ by $(\tilde{A}_{cl}, \tilde{B}_{cl}, \tilde{C}_{cl}, \tilde{D}_{cl})$. Let $X \triangleq vec(R_{block})$ and rewrite the above optimization problem as

$$\begin{aligned} & minX_1 \\ s.t. \quad & A_{eq}X = B_{eq}, \\ & P(X) < 0, \\ & X \geq 0, \end{aligned}$$

where $A_{eq}X = B_{eq}$ captures the equality constraints (2), $P(X) < 0$ captures constraints (3) and $X \geq 0$ are equivalent to constraints (4). For example, if $N = 4$, then

$$R_{block} = \begin{bmatrix} R_{00} & & & \\ R_{01} & R_{11} & & \\ R_{02} & R_{12} & R_{22} & \\ R_{03} & R_{13} & R_{23} & R_{33} \end{bmatrix},$$

$$X = \begin{bmatrix} R_{00} & R_{01} & R_{02} & R_{03} & R_{11} & R_{12} & R_{13} & R_{22} & R_{23} & R_{33} \end{bmatrix}',$$

$$A_{eq} = \begin{bmatrix} -1 & 1 & 0 & 0 & 1 & 0 & 0 & 0 & 0 & 0 \\ -1 & 0 & 1 & 0 & 0 & 1 & 0 & 1 & 0 & 0 \\ -1 & 0 & 0 & 1 & 0 & 0 & 1 & 0 & 1 & 1 \end{bmatrix},$$

$$B_{eq} = \begin{bmatrix} 0 & 0 & 0 \end{bmatrix}',$$

and

$$P(X) = ||\tilde{D}_{cl}F_4(X)||_1 + \sum_{k=1}^{n} ||\tilde{C}_{cl}\tilde{A}_{cl}^{k-1}\tilde{B}_{cl}F_4(X)||_1 - 1,$$

with

$$
\begin{aligned}
c_1' &= \begin{bmatrix} 1 & 1 & 1 & 1 & 0 & 0 & 0 & 0 & 0 & 0 \end{bmatrix} \\
c_2' &= \begin{bmatrix} 0 & 0 & 0 & 0 & 1 & 1 & 1 & 0 & 0 & 0 \end{bmatrix} \\
c_3' &= \begin{bmatrix} 0 & 0 & 0 & 0 & 0 & 0 & 0 & 1 & 1 & 0 \end{bmatrix} \\
c_4' &= \begin{bmatrix} 0 & 0 & 0 & 0 & 0 & 0 & 0 & 0 & 0 & 1 \end{bmatrix}.
\end{aligned}
$$

and

$$
F_4(X) = \begin{bmatrix} 2^{-c_1'X} & & & \\ & 2^{-c_2'X} & & \\ & & 2^{-c_3'X} & \\ & & & 2^{-c_4'X} \end{bmatrix}.
$$

Note that we approximate the 1-norm of $(I - \tilde{G}\tilde{K})^{-1}\tilde{G}\tilde{K}\tilde{F}_N$, to guarantee that we can numerically compute the solution to the constrained minimization problem.[2]

We now set $N = 4$, and solve for the most efficient quantizers that maintain FG stability for a variety of plant and controller pairs. As previously mentioned, when dealing with RB quantizers in the loop, the stability results derived hold when G and K are periodic with period N. We first assume that the plant and controller to be periodic systems with period N, to conduct preliminary sanity checks. We then construct examples for LTI plants and time-varying controllers generated from LTI controllers (as described in section 2.1.2). To solve for optimal bit-allocation strategies, we used MATLAB's function 'fmincon.m'.

Table 3.1 shows the resulting optimal R^*_{block} for different $\tilde{A}_{cl}$. We fix $\tilde{B}_{cl} = -I$, $\tilde{C}_{cl} = I$, and $\tilde{D}_{cl} = 0$. The minimum channel rate, R_{min}, required for stability for each corresponding closed-loop system is $R^*_{block}(1,1)$.

There are many observations that one can gleam from Table 3.1.

[2]To guarantee that the approximate 1-norm satisfies our stability condition, we require a finite-sum upper bound on the 1-norm of $(I - \tilde{G}\tilde{K})^{-1}\tilde{G}\tilde{K}\tilde{F}_N$, to satisfy the condition. See [9] for details on such an upper bound.

Table 3.1: Optimal Bit-Allocation Strategies For Various Closed-Loop Periodic Systems

$\tilde{\mathbf{A}}_{\mathbf{cl}}$	$\mathbf{R}^{*}_{\mathbf{block}}$
$\begin{bmatrix} 0.9 & & & \\ & 0.9 & & \\ & & 0.9 & \\ & & & 0.9 \end{bmatrix}$	$\begin{bmatrix} 4.32 & & & \\ & 4.32 & & \\ & & 4.32 & \\ & & & 4.32 \end{bmatrix}$
$\begin{bmatrix} 0.3 & & & \\ & 0.3 & & \\ & & 0.3 & \\ & & & 0.3 \end{bmatrix}$	$\begin{bmatrix} 1.51 & & & \\ & 1.51 & & \\ & & 1.51 & \\ & & & 1.51 \end{bmatrix}$
$\begin{bmatrix} 0.9 & & & \\ & 0.7 & & \\ & & 0.5 & \\ & & & 0.3 \end{bmatrix}$	$\begin{bmatrix} 3.47 & & & \\ 1.25 & 2.22 & & \\ 0.60 & 0.66 & 2.21 & \\ 0.09 & 0.43 & 0.37 & 2.58 \end{bmatrix}$

- If $\tilde{A}_{cl} = \rho I$, then the optimal R_{block} is diagonal. This is due to the fact that all components in the vector $\tilde{y}$ will be identical under zero initial conditions (since $\tilde{B}_{cl} = -I$). One may believe that a more intelligent strategy, in the case where all the components are identical, is to allocate all the bits to one of the components and have the decoder understand that all the components of $\tilde{y}$ take on the same value. However, this induces a delay of N time steps in the loop, which may impact stability.

- The larger the spectral radius of $\tilde{A}_{cl}$, the larger R_{min} must be for stability. Again, the component of $\tilde{y}$ that decays most slowly forces the channel to have larger rates for stability.

- If $\tilde{A}_{cl}$ is diagonal, with different diagonal components, then R_{block} is not necessarily diagonal. In particular, the optimal strategy tries to allocate more bits to the output components of $\tilde{y}$ that decay at slower rates, *i.e.,* those components that are functions of states that have eigenvalues with larger magnitudes. This is intuitive as the signals that decay more slowly are larger in magnitude over

Table 3.2: Optimal Bit-Allocation Strategies For Various Closed-Loop LTI Systems: R_{min} denotes the minimum rate required for stability when a TI memoryless $Q(\mathcal{R}, M)$-quantizer is in the loop.

$\mathbf{A_{cl}}$	$\mathbf{R^*_{block}}$	R_{min}
$\begin{bmatrix} 0.9 & & & \\ & 0.9 & & \\ & & 0.9 & \\ & & & 0.9 \end{bmatrix}$	$\begin{bmatrix} 9.19 & & & \\ 0.33 & 8.86 & & \\ & 0.15 & 9.04 & \\ & & & 9.19 \end{bmatrix}$	9.25
$\begin{bmatrix} 0.3 & & & \\ & 0.3 & & \\ & & 0.3 & \\ & & & 0.3 \end{bmatrix}$	$\begin{bmatrix} 6.99 & & & \\ 0.13 & 6.86 & & \\ 0.06 & 0.23 & 6.70 & \\ & & & 6.99 \end{bmatrix}$	7.08
$\begin{bmatrix} 0.9 & & & \\ & 0.7 & & \\ & & 0.5 & \\ & & & 0.3 \end{bmatrix}$	$\begin{bmatrix} 7.63 & & & \\ 0.22 & 7.41 & & \\ 0.16 & 0.33 & 7.14 & \\ & & & 7.63 \end{bmatrix}$	10.98

time and hence the quantizer is more likely to generate more errors on these signals if it fails to allocate sufficient bits to them.

Next, we consider examples where G is LTI and K is time-varying generated from K^{LTI}. In these cases, it is not as easy to see how certain inputs affect certain outputs during each time step.

Table 3.2 shows the resulting optimal R^*_{block} for different closed-loop systems. Again we allow A_{cl} to vary, and fix $B_{cl} = -[\ 1\ \ 2\ \ 1\ \ 10\ ]'$, $C_{cl} = [\ 1\ \ 5\ \ 3\ \ 1\ ]$, and $D_{cl} = 0$. We also consider memoryless quantizers ($N = 1$), *i.e.*, R bits are allocated to every input of the quantizer, for the same plants and controllers. In this case, $R_{min} > log_2(||TK^{LTI}||_1)$. The last column of Table 3.2 shows the minimum rate required for stability for memoryless quantizers.

When we compare the minimum rates for the finite-memory RB quantizers and memoryless quantizers, we see that forcing the quantizer to be memoryless requires the channel to have larger transmission rates to maintain FG stability. Therefore, stability may be achieved for channels with low rates by allowing the quantizer to have more memory.

3.3 Synthesizing Controllers

In this section, we show how one can synthesize a controller to track a family of sinusoidal commands, while minimizing the effects of the quantizer. Again we fix $E = Q_{RB}(\mathcal{R}, M)$ having block size N, and consider a family of reference inputs that consist of sinusoids with frequency-dependent amplitudes, *i.e.*, $\mathcal{C}_r = \{r | r = Wr_{pf}, ||r_{pf}||_\infty \leq 1\}$, where r_{pf} is any pre-filtered sinusoid input of amplitude ≤ 1, and W is a given real-rational stable transfer function.

If $r \in \mathcal{C}_r$, then r has an energy spectrum weighted by $\frac{1}{W(e^{j\omega})}$. For example, if W is a low-pass filter, then the energy spectrum of r is confined to low frequencies. In general, W "shapes" the energy spectrum of r. Recall, that if the conditions stated in Theorem 2.2.1 are satisfied, we get FG stability, *i.e.*,

$$||y||_\infty \leq ||T||_1||r||_\infty + m||TKF||_1,$$

which becomes

$$||y||_\infty \leq ||TW||_1||r||_\infty + \frac{||TW||_1}{1-||TKF||_1}||TKF||_1,$$

for this example. We call the second term, $\beta = \frac{||TW||_1 \, ||TKF||_1}{1-||TKF||_1}$, the quantizer "bias."

Suppose our performance objectives are as follows,

- Maintain FG stability: $||TW||_1 < \infty$ and $||TKF(\mathcal{R})||_1 < 1$.
- Minimize bias due to quantizer: minimize $||TKF(\mathcal{R})||_1$.
- Track r: minimize $||I - TW||_1$,

Then, since the encoder is a repeated-block quantizer, we can redefine the system in lifted coordinates to obtain an LTI description of the closed-loop system, and translate achieving these goals by solving the following optimization problem.

$$\begin{aligned} \min_{\tilde{K}} \quad & \left\| \begin{array}{c} (I - \tilde{T}\tilde{W}) \\ \tilde{T}\tilde{K}\tilde{F}_N(\mathcal{R}) \end{array} \right\|_1 \\ s.t. \quad & ||\tilde{T}\tilde{W}||_1 < \infty, \\ & ||\tilde{T}\tilde{K}\tilde{F}_N(\mathcal{R})|| < 1. \end{aligned} \tag{3.4}$$

A method for solving the above problem can be found in [9], and once the optimal $\tilde{K}$ is computed, one must check if the corresponding K is still LTI.

To simultaneously solve for the optimal bit-allocation strategy that will minimize the channel rate required for FG stability (and track r), and design a controller to minimize the bias, one can perform an "$\mathcal{R}$-K", iteratation procedure. The algorithm starts with an initial controller, $\mathcal{K}_0$, and then solves the following problem to construct $\mathcal{R}_0$:

$$\begin{aligned} & & minR \\ s.t. \quad R = 1 + \sum_j R_{ij} \quad & i = 0, 2, .., N-1, & (3.5) \\ ||(I - \tilde{G}\tilde{K}_0)^{-1}\tilde{G}\tilde{K}_0\tilde{F}_N||_1 < 1, & & (3.6) \\ R_{ij} \geq 0 \quad j \leq i = 0, 2, .., N-1, & & (3.7) \end{aligned}$$

Then once R_0 is computed, it is fixed and K_1 is computed by solving

$$\begin{aligned} \min_{\tilde{K}} \quad & \left\| \begin{array}{c} (I - \tilde{T}\tilde{W}) \\ \tilde{T}\tilde{K}\tilde{F}_N(\mathcal{R}) \end{array} \right\|_1 \\ s.t. \quad & ||\tilde{T}\tilde{W}||_1 < \infty, \\ & ||\tilde{T}\tilde{K}\tilde{F}_N(\mathcal{R}_0)|| < 1. \end{aligned} \tag{3.8}$$

The algorithm continues to iterate between the two optimization problems until both

costs fail to change much. This of course does not necessarily lead to the global optimal controller and rate matrix, as the solutions depend on the initial condition of the iteration process.

3.4 Dynamic Quantization

The $(\mathcal{R}, M)$-quantizer studied in this thesis is *static* in that it is an operator that cannot be described by states and state-evolution equations that depend on its inputs. We define a quantizer to be *dynamic* if it has states that evolve as a function of the inputs. In this section, we show how linear dynamic quantization does not improve over static $\mathcal{R}$-M quantization, for the class of encoders considered in this thesis.

Specifically, we analyze the quantizer, shown in Figure 3-2, where H is a linear, stable, dynamic, invertible, and causal operator with $||H^{-1}||_1 = 1$, and Q is an $(\mathcal{R}, M)$-quantizer with a diagonal rate matrix, $\mathcal{R} = (R-1)I$, and a scale matrix $M = mI$. Since H is a linear dynamic operator, we call this encoder a *linear dynamic quantizer.*

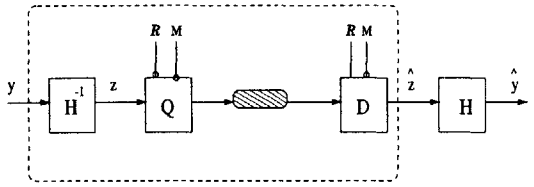

Figure 3-2: Linear Dynamic Quantizer

The closed loop model with a linear dynamic quantizer in the loop is shown in Figure 3-3.

From Figure 3-3, we see that $y_{DQ} = Tr + 2^{-R+1}mTKHe$, where $||e||_\infty \leq 1$, and $z = H^{-1}T + 2^{-R+1}mTKe$. It is easy to verify that the sufficient conditions for stability for the closed-loop system with a dynamic quantizer in the loop are not impacted by H. However H does impact the bias term due to the quantization error. Specifically, $||y_{DQ}||_\infty \leq ||T||_1||r||_\infty + m2^{(1-R)}||TKH||_1$. If we choose $m \geq \frac{||H^{-1}T||_1\bar{r}}{1-2^{1-R}||TK||_1} \geq 0$, which

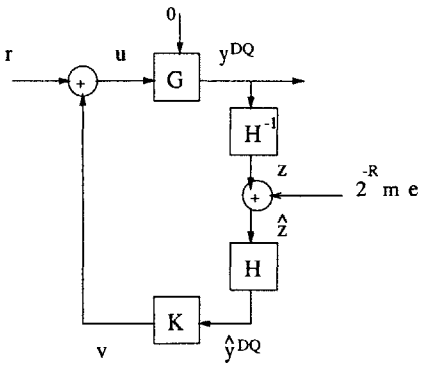

Figure 3-3: Closed Loop Model with Dynamic Quantizer

is possible given the norm bounds on r, T, and TK, then the quantizer is valid. *i.e.*, $||z||_\infty \leq m$. Therefore, the minimum possible bias, β_{min}, for any H is obtained by solving the following minimization problem.

$$\min_H \frac{2^{1-R}||TKH||_1||H^{-1}T||_1\bar{r}}{1-2^{1-R}||TK||_1}$$

s.t. H is a linear, stable, dynamic, invertible, causal, and $||H^{-1}||_1 = 1$.

We disregard terms independent of H, and compute a lower bound for $||TKH||_1||H^{-1}T||_1$. It is easy to show that $||H^{-1}T||_1 \geq \frac{||T||_1}{||H||}$, and $||TKH||_1 \geq \frac{||TK||_1}{||H^{-1}||_1} = ||TK||_1$. This implies that $||TKH||_1||H^{-1}T||_1 \geq \frac{||T||_1}{||H||_1}$. The minimum bias term with dynamic quantization is the minimum bias term without quantization divided by $||H||_1$. Since $||H^{-1}||_1 = 1$, we get that $||H||_1 \geq 1$, which indicates that dynamic quantizers may give rise to smaller biases. This will be further explored in future work.

3.5 Summary

In summary, for the simple feedback network, we studied a new class of encoders that have memory but do not have access to the control input to the plant. If the encoder is not local to the plant and if it does not know what controller will receive the signal it sends through the channel, then it can be modeled as belonging to this class. We constructed a parameterization of time-varying quantizers that belong to this

encoder class, and that leads to a convex characterization of bit-allocation strategies that maintain finite-gain stability. For finite memory quantizers, the convex characterization of stabilizing quantizers allows for efficient and non-trivial bit-allocation strategies to be synthesized for a given plant and controller. Finally, we showed how our simple use of input-output theory leads to computable formulations of controller synthesis problems under finite-rate feedback.

Chapter 4

Finite-Rate Feedforward Control: Performance Limitations

In this chapter, we consider a simple feed-forward network and two finite horizon performance objectives. The first objective is to minimize a weighted tracking error between the remote system output and the reference command over a finite number of time steps. The second objective is to navigate the state of the remote system from a nonzero initial condition to as close to the origin as possible in minimum number of time steps. We derive performance limitations for both objectives by computing lower bounds on each metric. We also construct coding schemes to compute upper bounds. Finally, we compare our set up and results for the navigation problem to similar previous work.

4.1 Finite-Horizon Tracking

In this section, we are interested in tracking a class of reference commands over a finite-horizon and under finite-rate constraints. We consider the cascade of SISO discrete-time systems shown in Figure 4-1.

Specifically,

- $w \in \mathbb{R}^T$ *s.t.* $||w||_2 \leq 1$,

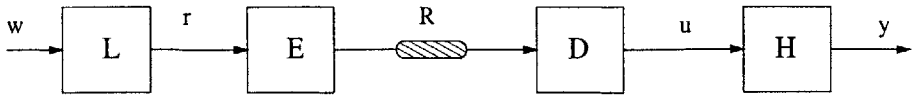

Figure 4-1: Finite Horizon Tracking Set Up

- $L : \mathbb{R}^T \to \mathbb{R}^T$ is an invertible linear operator,
- $E : \mathbb{R}^T \to \{0,1\}^{RT}$ is an arbitrary operator (encoder) that maps a real vector to a sequence of 2^{RT} binary symbols,
- R is the channel rate for the finite-rate noiseless channel that maps $\{0,1\}^{RT} \to \{0,1\}^{RT}$,
- $D : \{0,1\}^{RT} \to \mathbb{R}^T$ is an arbitrary operator (decoder) that maps a sequence of 2^{RT} binary symbols to a real vector, and
- $H : \mathbb{R}^T \to \mathbb{R}^T$ is an invertible linear operator.

Note that L defines a class of signals, $\mathcal{C}_r$, that is generated from a unit ball in $\mathbb{R}^T$. Since L is linear, it maps the unit ball to a bounded ellipsoid (see Theorem 4.1.1 for details). We set out to minimize a tracking error over all signals in this class (worst-case analysis). Since the input and output signals have finite length, the following performance metric is computed over a finite-horizon:

$$||W(y-r)||_2^2,$$

where $W \in \mathbb{R}^T \times \mathbb{R}^T$ is a given weight matrix. Since L and H are both invertible operators, in the ideal case of perfect communication ($R = \infty$), it is possible to construct an encoder and decoder such that $||W(y-r)||_2^2 = 0 \quad \forall r \in \mathcal{C}_r$. However, with a finite-rate constraint, the control, u, can only take 2^{RT} values over a horizon of T time steps. Therefore, it is not clear what level of performance is achievable.

To understand the limitations of finite-rate feedforward control, we are interested computing γ_{LB} and γ_{UB}, such that

$$\gamma_{LB} \leq \sup_{r \in \mathcal{C}_r} ||W(y-r)||_2^2 \leq \gamma_{UB}.$$

Knowledge of γ_{LB} tells us that regardless of the encoder and decoder that we select, we can do no better than this lower bound. Therefore, we expect it to be a function of R, T, L, and W (independent of E and D). The upper bound tells us that there exists a coding scheme (and encoder an decoder) such that the worst case performance is always less than or equal to γ_{UB}. Therefore, to compute γ_{UB}, we need to construct an encoder and decoder and compute the corresponding worst-case performance. We compute γ_{LB} and γ_{UB} in the following two sections.

4.1.1 A Lower Bound

In this section we derive the lower bound on worst-case performance.

Theorem 4.1.1. *Assume that* $det(W) \neq 0$, $det(L) \neq 0$, [1] *and* H *is a one-to-one mapping. Then,*

$$\gamma_{LB} = 2^{-2R}\{|det(L)|\ |det(W)|\}^{\frac{2}{T}}.$$

Proof.

The set of all possible commands, $\mathcal{C}_r \triangleq \{r \in \mathbb{R}^T | r = Lw, w'w \leq 1\} = \{r \in \mathbb{R}^T \mid (L^{-1}r)'(L^{-1}r) \leq 1\}$. $\mathcal{C}_r$ *is a bounded ellipsoid in* $\mathbb{R}^T$ *centered at the origin with volume* $\eta\ det\{((L^{-1})'(L^{-1}))^{-0.5}\} = \eta|det(L)|$, *where* η *is the volume of a unit ball in* $\mathbb{R}^T$.

Over a horizon T, *the channel sends a total of* RT *bits which limits the control signal to take on no more than* 2^{RT} *values; and, since* H *is a one-to-one mapping, the channel limits the output to take on no more than* 2^{RT} *values.*

Consider a selection of outputs $y_1, y_2, ..., y_{2^{RT}}$, *which correspond to inputs* $u_1, u_2, ..., u_{2^{RT}}$, *respectively. We must then map each* $r \in \mathcal{C}_r$ *to exactly one* y_i $i = 1, 2, ..., 2^{RT}$. *Such a mapping induces a partition on* $\mathcal{C}_r$. *In particular, define* $P_i = \{r \in \mathcal{C}_r |\ r \rightarrow y_i\}$ *for* $i = 1, 2, ..., 2^{RT}$. *Now, suppose that the selection* $y_1, y_2, ..., y_{2^{RT}}$ *were chosen such*

[1] *The lower bound can still be computed if one or both of these assumptions are not true. The proof is identical to the one given here, but is performed in a smaller dimensional space.*

that $||W(y_i - r)||_2^2 \leq \gamma$ *for all* $r \in P_i$, *and for all* i. *Then necessarily* $P_i \subseteq S_{y_i}^{\gamma} \triangleq \{r \in \mathbb{R}^T \mid (r - y_i)'W'W(r - y_i) \leq \gamma\}$. *Note that* $S_{y_i}^{\gamma}$ *is a bounded ellipsoid in* $\mathbb{R}^T$ *centered at point* y_i *with volume* $\eta(\sqrt{\gamma})^T det\{(W'W)^{-0.5}\} = \frac{\eta\sqrt{\gamma}^T}{|det(W)|}$. *See Figure 4-2 for an illustration.*

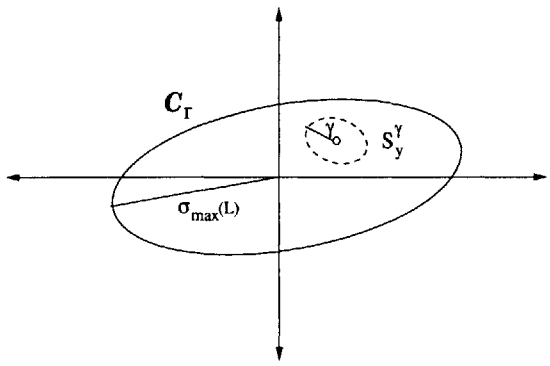

Figure 4-2: Bounded Ellipsoids C_r *and* S_y^{γ}

Since $P_i \subseteq S_{y_i}^{\gamma}$ *for each* $i = 1, 2, ..., 2^{RT}$, *it is necessary that* 2^{RT} *bounded ellipsoids* (S_y^{γ}) *cover the set* C_r. *This implies that* $2^{RT} \times volume(S_y^{\gamma}) \geq volume(C_r)$. *Equivalently,*

$$2^{RT} \geq \frac{volume(C_r)}{volume(S_y^{\gamma})} = \frac{|det(L)|\ |det(W)|}{(\sqrt{\gamma})^T}.$$

After rearranging terms, we get that $\gamma \geq 2^{-2R}\{|det(L)|\ |det(W)|\}^{\frac{2}{T}}$.

■

Since we often consider classes of inputs generated from LTI systems, *i.e.*, L is LTI, we compute the lower bound for this case in the following corollary.

Corollary 4.1.1. *Assume that* $det(W) \neq 0$, $det(L) \neq 0$, *and* H *is a one-to-one mapping. If* L *is a causal SISO LTI system with state-space description* $L = ss(A_l, B_l, C_l, D_l)$, *then*

$$||W(y - r)||_2^2 \geq 2^{-2R}(D_l)^2\{|det(W)|\}^{\frac{2}{T}}.$$

Proof. *If* L *is a SISO causal LTI with state-space description* $L = ss(A_l, B_l, C_l, D_l)$, *then for* T *time steps, it can be represented as a* $T \times T$ *lower triangular Toeplitz matrix*

operator, with all T eigenvalues equal to D_l. This implies that the $\{det(L)\}^{\frac{2}{T}} = (D_l)^2$.

■

We now make some comments about γ_{LB}.

- γ_{LB} depends on L (class of reference commands), W (performance weights), T (performance horizon), and R (channel rate).
- If $det(W)$ and/or if $det(L) = 0$, then the counting argument shown in Theorem 4.1.1 has to be done in $\mathbb{R}^s$, where $s = \min\{rank(L), rank(W)\}$. Consider a case where $W = diag(\lambda_0, \lambda_1, ..., \lambda_{T-1})$, and $det(W) = 0$ because $\lambda_{k_0} = 0$, for some $0 \leq k_0 \leq T-1$. Then, 0 bits can be allocated to r_{k_0} and performance will not be impacted. Therefore, the problem reduces to allocated bits to r_k for all $k \neq k_0$. On the other hand, if $det(L) = 0$ then one or more of the r_k's are linear combinations of each other, and bits only need to be allocated to one of these r_k's, and the decoder can reconstruct the others knowing L.
- If L is LTI and if $W = I$, then γ_{LB}, is independent of T.
- It is helpful (as we will see when we compute upper bounds) to rewrite the lower bound in terms of the singular and eigenvalues of the matrix WL as follows:

$$\gamma_{LB} = 2^{-2R}\{\prod_{i=0}^{T-1} \sigma_i\}^{\frac{2}{T}} = 2^{-2R}\{\prod_{i=0}^{T-1} |\lambda_i|\}^{\frac{2}{T}}.$$

4.1.2 Causality

In this section, we discuss how the structure of each operator in the tracking system is impacted by assuming causality.

- **L**: Since L is linear, it can be represented as a matrix operator of size $T \times T$. If we further assume that it is also causal, then its matrix representation will be lower triangular. This implies that r_k only depends on w_j for $j \leq k$.
- **E**: At time step k, E has received $r_0, r_1, ..., r_k$, and transmits R bits which represent information only about $r_0, r_1, ..., r_k$. Note that at time step k a total of kR bits have been sent to the decoder.

- **Finite-Rate Channel**: The channel always send R bits per time step regardless of whether the surrounding operators are causal or noncausal.
- **D**: At time step k, the decoder processes the kR bits it has received since time 0 to produce control value u_k.
- **H**: Since H is linear, it can be represented as a matrix operator of size $T \times T$. If we further assume that it is also causal, then its matrix representation will be lower triangular. This implies that y_k only depends on u_j for $j \leq k$.

We highlight causality, because in practice we deal with causal systems. In the previous section, we derived a lower bound that did not assume causality of any component in the cascaded system. Therefore, the lower bound may be far from what is achievable in practice. Nevertheless, it shows us that one cannot design an encoder and decoder that will do better than γ_{LB}. The lower bound also allows us to compare to noncausal and causal upper bounds, which we compute in the following two sections.

4.1.3 Noncausal Upper Bound

In this section, we derive an upper bound on worst-case performance assuming that the operators may be noncausal. The upper bound is derived using a coding scheme that transmits information about the vector r in terms of a basis derived from the singular value decomposition (SVD) of the matrix WL. Consider Figure 4-3 below. The encoder first uses the SVD of $WL = U\Sigma V^*$ to write $Wr = \sum_{i=0}^{T} \sigma_i \alpha_i u_i$, where σ_i is the ith singular value of WL, $\alpha_i = v_i^* w$ where v_i^* is the ith row vector of V^*, and u_i is the ith column vector of U. The α_i's are then each converted into their binary representations and truncated according to the bit-allocation strategy denoted in $\mathcal{R} = (R_0, R_1, ..., R_{T-1})$. In particular, a total of R_k bits are allocated to α_k, for $k = 0, 1, ..., T$, and the only restriction is that $\sum_{k=0}^{T} R_k = TR$.

The decoder uses the bit-allocation strategy $\mathcal{R}$ to reconstruct α and then uses the SVD of WL to compute $\hat{r}$ from $\hat{\alpha}$. Finally, the decoder applies H^{-1} to $\hat{r}$ to generate u. We call this $E - D$ construction the "SVD Coding Scheme."

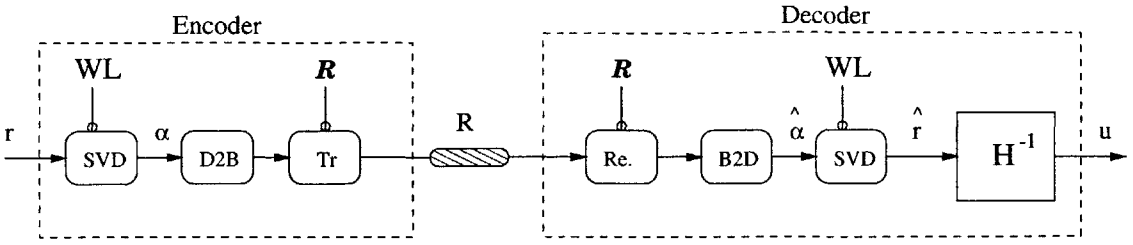

Figure 4-3: SVD Coding Scheme

Note that with the above SVD coding scheme, $||W(y-r)||_2^2 = ||W(\hat{r}-r)||_2^2 = ||WL(\hat{w}-w)||_2^2 = \sum_{i=0}^{T-1}\sum_{j=0}^{T-1}(\hat{\alpha}_i-\alpha_i)(\hat{\alpha}_j-\alpha_j)\sigma_i\sigma_j(u_i'u_j) \leq \sum_{i=0}^{T-1}|\alpha_i|^2 2^{-2R_i}\sigma_i^2 \leq \sum_{i=0}^{T-1}2^{-2R_i}\sigma_i^2$.

To derive the upper bound using the above SVD coding scheme, we construct $\mathcal{R} = (R_0, R_1, ..., R_{T-1})$ to solve the following optimization problem:

$$\begin{aligned} &\min \textstyle\sum_{i=0}^{T-1} 2^{-2R_i}\sigma_i^2 \\ &\text{s.t. } \textstyle\sum_{i=0}^{T} R_i = TR. \end{aligned}$$

We allow the rates to take on non-integer values to solve for an optimal bit-allocation strategy. The resulting non-integer valued rates can be interpreted as average rates over time. The above problem is computable and it is easy to verify (using Lagrange multipliers) that the optimal solution is $R_i^* = (R - \frac{1}{T}\sum_{i=0}^{T-1} log_2(\sigma_i)) + log_2(\sigma_i)$. Therefore, the larger the singular value σ_i, the larger R_i, *i.e.*, the more bits are allocated to α_i. The resulting upper bound is $\sum_{i=0}^{T-1}2^{-2R_i^*}\sigma_i^2 = \sum_{i=0}^{T-1}2^{-2(\frac{-1}{T}\sum_{i=0}^{T-1}log_2(\sigma_i)+R)} = T2^{-2R}\prod_{i=0}^{T-1}(\sigma_i)^{\frac{2}{T}}$. Recall that $|det(WL)| = \prod_{i=0}^{T-1}(\sigma_i) = |det(L)|\ |det(W)|$. This give us $\gamma_{UB} = T2^{-2R}\{|det(L)|\ |det(W)|\}^{\frac{2}{T}} = T\gamma_{LB}$.

Therefore, if the operators are, in general, noncausal we get that

$$\gamma_{LB} \leq \sup_{r\in\mathcal{C}_r} ||W(y-r)||_2^2 \leq T\gamma_{LB}.$$

It is interesting that two different approaches for computing the lower and upper bounds led to worst-case performance that are related to each other by a factor of T! In section 4.1.5, we see how the lower and the noncausal upper bound compare to

each other for different performance weights and L matrices, *i.e.*, different classes of commands.

Finally, it is also interesting to note that the minimization problem above that gives rise to the noncausal upper bound is very similar to that of finding the optimal prefix code with minimum expected length in information theory [16]. In information theory, each codeword c_i of a codebook has integer length l_i and is generated with probability p_i. Thus, the expected length is $\sum_{i=1}^{\infty} l_i p_i$. For a code to be a "prefix" code (no codeword is a prefix of any other codeword and is therefore uniquely decodable), Kraft's inequality must be satisfied, which states that $\sum_{i=1}^{\infty} 2^{-l_i} \leq 1$. A simple analysis by calculus gives a the optimal non-integer code lengths $l_i^* = -log_2(p_i)$. Here the more probable a codeword, the shorter the length should be. The analogy is that the inverse of the singular values, σ_i^{-1}, play the role of the probabilities of codewords, p_i.

4.1.4 Causal Upper Bound

In this section, we derive a coarse upper bound assuming that the encoder and decoder are both causal and implement a coding scheme illustrated in Figure 4-4. Causality forces the encoder to receive r_k at time step k for all $k = 0, 1, ..., T-1$. The encoder first divides r_k by $\sigma_{max}(L(k,:))$, where $\sigma_{max}(L(k,:))$ is the maximum singular value of the kth row vector of L. This ensures that $|z_k| \leq 1$. Then, the encoder allocates R bits to the binary representation of z_k and transmits it across the channel. The decoder construct $\hat{z}_k$ and multiplies it by $\sigma_{max}(L(k,:))$ to produce $\hat{r}_k$ at time k. Finally, the decoder applies H^{-1} to $\hat{r}$ to generate control u. For simplicity, we consider $W = diag(\lambda_0, \lambda_1, ..., \lambda_{T-1})$ where without loss of generality $|\lambda_i| \leq 1$, $\forall i$. We then get that $||W(y-r)||_2^2 = ||W(\hat{r}-r)||_2^2 \leq 2^{-2R} \sum_{i=0}^{T-1} \lambda_i^2 \sigma_{max}(L(i,:))^2$.

4.1.5 Comparison of Lower and Upper Bounds

We now compare the noncausal and causal upper bounds to each other and to the lower bound from section 4.1.1 for different LTI causal systems $L = ss(A_l, B_l, C_l, D_l)$, and for different time horizons T. We consider diagonal weight matrices $W = diag(\lambda_0, \lambda_1, ..., \lambda_{T-1})$

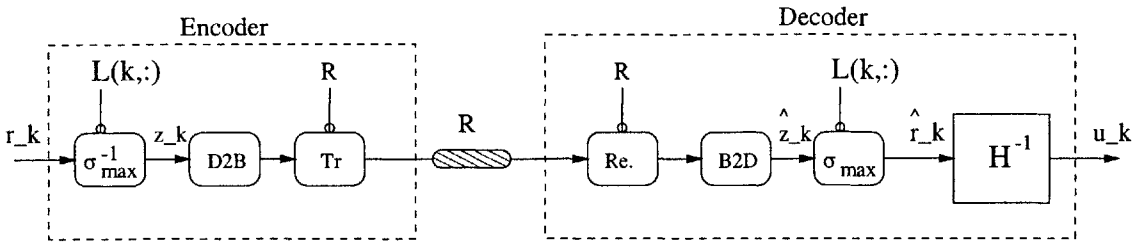

Figure 4-4: Causal Coding Scheme

with $|\lambda_i| \leq 1$, $\forall i$, and fix the rate $R = 10$. Under such conditions, we note that

$$\gamma_{LB} = 2^{-2R}(D_l)^2\{\prod_{i=0}^{T-1}|\lambda_i|\}^{\frac{2}{T}}.$$

Figures 4-5 and 4-6 illustrate the bounds for the 2-norm or energy of the weighted tracking error ($||W(y-r)||_2^2$) and the bounds for the *power* ($\frac{1}{T}||W(y-r)||_2^2$) of the weighted tracking error for the following scenarios.

1. $L = ss(0.9, 0.9, 1, 1)$, and λ_i for $i = 0, 1, ..., T-1$, are experimental outcomes of i.i.d. random variables generated by taking experimental outcome from normal Gaussian distributions and then dividing each by its norm.

2. $L = ss(0.5, 0.5, 1, 1)$, and λ_i for $i = 0, 1, ..., T-1$, are experimental outcomes of i.i.d. random variables generated by taking experimental outcome from normal Gaussian distributions and then dividing each by its norm.

3. $L = ss(0.9, 0.9, 1, 1)$, and $\lambda_i = (0.5)^i$ for $i = 0, 1, ..., T-1$.

4. L is noncausal and generated by taking the LTI system $ss(0.9, 0.9, 1, 1)$, and adding it to its transpose, λ_i for $i = 0, 1, ..., T-1$, are experimental outcomes of i.i.d. random variables generated by taking experimental outcome from normal Gaussian distributions and then dividing each by its norm.

We make a few observations from Figures 4-5 and 4-6.

- When the eigenvalues of W are chosen randomly from an i.i.d. process, then we see that the lower bound plateaus for large T. To see why this makes sense,

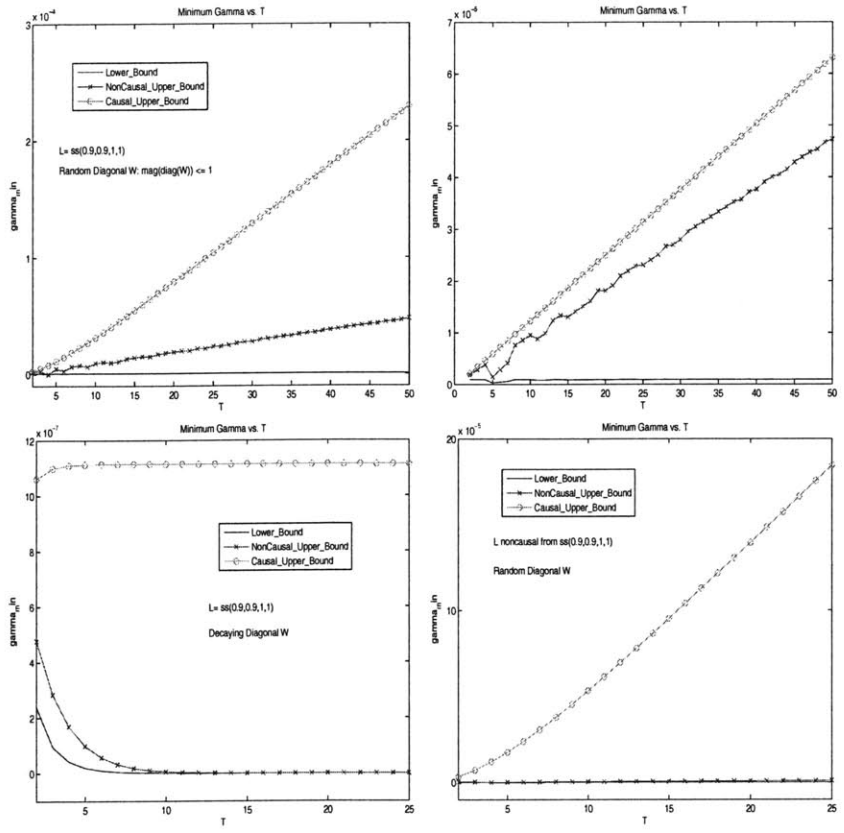

Figure 4-5: Top Left: Bounds for $L = ss(0.9, 0.9, 1, 1)$ and random weights, Top Right: Bounds for $L = ss(0.5, 0.5, 1, 1)$ and random weights, Bottom Left: Bounds for $L = ss(0.9, 0.9, 1, 1)$ and decaying weights, Bottom Right: Bounds for L noncausal generated from $ss(0.9, 0.9, 1, 1)$ and random weights

we compute the expected value and variance of γ_{LB} with $L = ss(0.9, 0.9, 1, 1)$ and observe their behaviour for large T.

$$E\{\gamma_{LB}\} = 2^{-2R} E\{\textstyle\prod_{i=0}^{T-1} |\lambda_i|^{\frac{2}{T}}\}.$$

Since the λ_i's are all independent, we get that the expectation of the product is the product of the expectations. In addition, since the λ_i's are identically distributed their expectations are all equal, and we get the following.

$$E\{\gamma_{LB}\} = 2^{-2R} \textstyle\prod_{i=0}^{T-1} E\{|\lambda_i|^{\frac{2}{T}}\} = 2^{-2R} E^T\{|\lambda|^{\frac{2}{T}}.$$

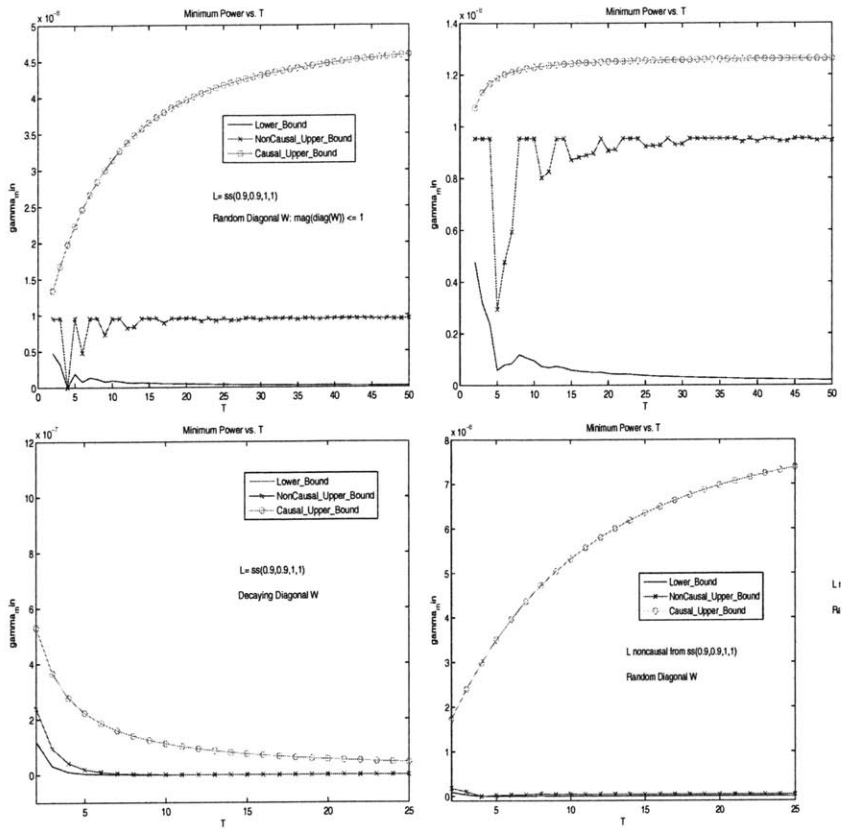

Figure 4-6: Top Left: Bounds for $L = ss(0.9, 0.9, 1, 1)$ and random weights, Top Right: Bounds for $L = ss(0.5, 0.5, 1, 1)$ and random weights, Bottom Left: Bounds for $L = ss(0.9, 0.9, 1, 1)$ and decaying weights, Bottom Right: BouXSnds for L noncausal generated from $ss(0.9, 0.9, 1, 1)$ and random weights

Now, as $T \to \infty$, we get that $E\{\gamma_{LB}\} \to 2^{-2R}$ since $|\lambda_i| \leq 1$. Next, we compute the variance of γ_{LB} by first computing $E\{\gamma_{LB}^2\}$.

$$E\{\gamma_{LB}^2\} = 2^{-4R} E\{\prod_{i=0}^{T-1} |\lambda_i|^{\frac{4}{T}}\} = 2^{-4R} E^T\{|\lambda|^{\frac{4}{T}}\}.$$

We see that as $T \to \infty$, we get that $E\{\gamma_{LB}^2\} \to 2^{-4R}$, which implies that $var(\gamma_{LB}) = E\{\gamma_{LB}^2\} - E^2\{\gamma_{LB}\} \to 0$. Therefore, for large T, we expect that the lower bound approaches 2^{-2R}.

- When the eigenvalues of W are exponentially decaying, *i.e.*, $\lambda_i = (0.5)^i$ for $i = 0, 1, ..., T-1$, then the lower bound and therefore noncausal upper bound

approach 0 as $T \to \infty$. This can be verified by showing that the ratio between the lower bound at time $T+1$ and at time T is less than 1, which shows that the lower bound is strictly decreasing as a function of T.

$$\frac{\gamma_{LB}(T+1)}{\gamma_{LB}(T)} = \frac{\{\prod_{i=0}^{T} \beta^i\}^{\frac{2}{T+1}}}{\{\prod_{i=0}^{T-1} \beta^i\}^{\frac{2}{T}}} = \beta < 1.$$

- The noncausal and causal upper bounds are closer to each other when the pole of the LTI system of L or that which generates a noncausal L is close to the origin than if the pole is close to the unit disk.

- When L is noncausal and the pole of the LTI system that generates L approaches the unit disk, the noncausal upper bound approaches the lower bound as T increases. In fact, if WL has one dominant singular value, σ_0, then the performance of this upper bound approaches γ_{LB}. In this case, we essentially only have one none zero value α_0 to send through the channel as the rest of the α_i's correspond to singular values that are close to 0. This implies that both bounds decay like 2^{-RT} and approach 0 as T gets large.

4.2 Finite-Horizon Navigation

In this section we assume that the remote system has some unknown initial condition x_0 which lies in a known set in $\mathbb{R}^n$. We want to steer the state of the remote system as close to the origin as possible under the constraint that the control input can take on at most 2^{RT} values after T time steps. For analysis, we consider the discrete-time system shown in Figure 4-7.

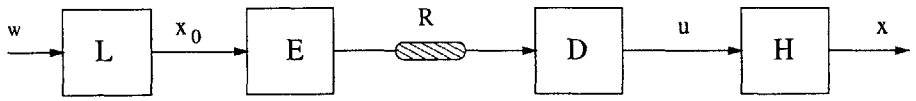

Figure 4-7: Finite Horizon Navigation Set Up

This is essentially the same set up as that introduced in section 4.1 with

- $w \in \mathbb{R}^n$ *s.t.* $||w||_2 \leq 1$,
- $L : \mathbb{R}^n \rightarrow \mathbb{R}^n$ is a linear operator,
- $x_0 \in \mathbb{R}^n$ is the initial state vector of system H,
- $E : \mathbb{R}^n \rightarrow \{0,1\}^{RT}$ is an arbitrary operator (encoder) that maps a real vector to a sequence of 2^{RT} binary symbols,
- R is the channel rate for the finite-rate noiseless channel that maps $\{0,1\}^{RT} \rightarrow \{0,1\}^{RT}$,
- $D : \{0,1\}^{RT} \rightarrow \mathbb{R}^T$ is an arbitrary operator (decoder) that maps a sequence of 2^{RT} binary symbols to a real vector, and
- H is a causal SISO LTI system with state-space representation $H = ss(A, B, I, 0)$.

Our goal is to minimize the time it takes for the state vector to reach an ellipsoid bounded by γ. Therefore, we fix γ and then look for the smallest T to meet performance, which is measured as

$$||x_{T-1}||_2^2 \leq \gamma.$$

We get the following equivalent representation of performance.

$$||Mu + A^{T-1}x_0||_2^2 \leq \gamma,$$

where A^{T-1} is the $(T-1)^{th}$ power of the matrix A, and $M = \begin{bmatrix} A^{T-2}B & A^{T-3}B & \dots & AB & B \end{bmatrix}$ is the reachability matrix of system H. Assume that the system is reachable, therefore, for $T \geq n$, M has full rank is a one-to-many mapping in general. We now compute T_{min} such that $||Mu + A^{T-1}x_0||_2^2 \leq \gamma$, for any given $\gamma > 0$.

4.2.1 A Lower Bound

In this section we derive a lower bound for T as a function of γ. We note that the metric $||Mu + A^{T-1}x_0||_2^2 \leq \gamma$ is identical to our previous tracking metric of $||Hu - Lw||_2^2 \leq \gamma$,

where $H \rightarrow M$ and $L \rightarrow -A^{T-1}\ L$. However, it is important to note that w and L are independent of T! After making these substitutions and applying Theorem 4.1.1, we get that

$$T \geq \left| \frac{2(log_2(|det(L)|) - log_2(|det(A)|)}{log_2(\gamma) + 2R - 2log(|det(A)|)} \right|.$$

Note that the lower bound depends on R, L, γ, and the system dynamics A.

4.2.2 Previous Work on Finite Horizon Navigation

In this section, we describe a similar navigation problem solved by Fagnani and Zampieri [14, 15] and then extended by Delvenne [11]. Another navigation set up that explores the tradeoffs between performance and control complexity for finite automata systems is given in [4].

In [15], Fagnani etal. consider the closed-loop system shown in Figure 4-8.

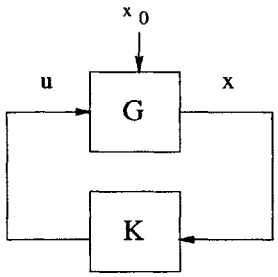

Figure 4-8: Closed-Loop System

The model of the closed-loop system (using the same notation as in [15]) is

$$G : x_{t+1} = Ax_t + Bu_t$$

$$K : \begin{cases} s_{t+1} = f(s_t, x_t) \\ u_t = k(s_t, x_t), \end{cases}$$

where $x_t \in \mathbb{R}^n$, $u_t \in \mathbb{R}$, $A \in \mathbb{R}^{n \times n}$, and $B \in \mathbb{R}^{n \times 1}$, $s \in S$ where S is a finite set of size M, $f : S \times \mathbb{R}^n \rightarrow S$, and $k : S \times \mathbb{R}^n \rightarrow \mathbb{R}$.

Furthermore, the controller is quantized in that there exists a finite family $\mathcal{K}_s = \{K_s^1, K_s^2, ..., K_s^N\}$ of disjoint subsets of $\mathbb{R}^n$ that cover $\mathbb{R}^n$, and such that the map $k(s,.)$ is constant on each K_s^j. Note that since S is finite, then the map $f(s,.)$ will also be quantized. That is, for each $s \in S$, there exists a finite family $\mathcal{F}_s = \{F_s^1, F_s^2, ..., F_s^M\}$ of disjoint subsets of $\mathbb{R}^n$ that cover $\mathbb{R}^n$, and such that the map $f(s,.)$ is constant on each F_s^j. Finally the initial state $x_0 \in W$, where W is some known bounded set in $\mathbb{R}^n$.

Fagnani etal. show that the above system is equivalent to that shown in Figure 4-9, where the encoder, E, and the decoder, D, are separated by a finite-rate noiseless channel that transmits R bits per time step, where $2^R = N$.

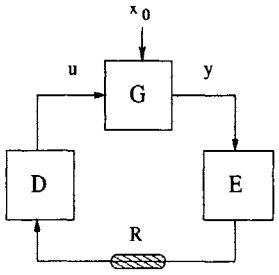

Figure 4-9: Equivalent Closed-Loop System

The encoder and decoder are described below.

- $E : \mathbb{R}^n \to \mathbf{Z}^+ \times \mathbf{Z}^+$ is the following dynamic operator:

$$E : \begin{cases} s_{t+1} = f(s_t, x_t) \\ (i_t, j_t) = q(s_t, x_t) \end{cases}$$

  We note that s is a $L \times 1$ vector, and defines the "complexity" of the encoder. The map q is defined as $q : S \times \mathbb{R}^n \to \mathbf{Z}^+ \times \mathbf{Z}^+$ such that $q(s,x) = (i,j)$ if and only if $x \in F_s^i \times K_s^j$.

- $D : \mathbf{Z}^+ \times \mathbf{Z}^+ \to \mathbb{R}$ is the following dynamic operator:

$$D = \begin{cases} s_{t+1} = \overline{f}(s_t, i_t, j_t) \\ u_t = \overline{k}(s_t, i_t, j_t), \end{cases}$$

such that $f = \overline{f} \circ q$, and $k = \overline{k} \circ q$.

With the above set up, Fagnani etal. ask the following question:

Given a subset V of W, and given that x_0 is a random vector that is uniformly distributed over W, find the minimum expected time, $E\{T_{(W,V)}\}$ that "traps" the state x_t in V for all $t \geq T$.

Fagnani etal. show that for a fixed value of M (the size of the set S), and any given $\beta > 0$,

$$\frac{E\{T_{(W,V)}\}}{ln(C)} \leq \beta \Rightarrow \frac{LN}{ln(C)} \leq \delta(\beta),$$

where $C = \frac{\mu[W]}{\mu[V]}$ (μ is the Lebesgue measure in $\mathbb{R}^n$.) is a contraction rate that describes how small the target set is with respect to the starting set. Also $\delta(\beta) = H_1 \beta w^{\frac{1}{\beta}}$, for some $w > 1$ and constant H_1, which depends on the plant dynamics. See [15] for details. This result shows a clear tradeoff between the complexity of the controller (L) and performance $E\{T_{(W,V)}\}$.

We now highlight the differences between our tracking problem discussed in section 4.1 and the problem described in this section [15].

- In [15], the objective is to not only reach V in minimum number of time steps, but the state must *stay* in V thereafter. Whereas, in our tracking problem, we want the state to reach a set (say V) in the minimum number of time steps, and do not specify what happens after time $t > T$.

- Another important distinction, is that the control u in [15] is a function of the system state x (feedback is used). Whereas, in our set up, the control input u only depends on x_0 and the set in which it lies.

- To compute our lower bound, we do not make any assumptions of the encoder and decoder, and the bound depends on the channel rate, the initial condition set, the final set, and the plant dynamics. In [15] the encoder and decoder are assumed to have equimemory, *i.e.,* both E and D can compute the state

s_t for all t, and their bound depends on the plant dynamics, channel rate, the initial condition set, the final set, *and* the complexity of the coding scheme (the number of states in encoder and decoder).

- Finally, our set up is deterministic and finds performance limitations in the worst case setting (over all x_0 in some bounded ellipsoid), whereas the formulation in [15] assumes that x_0 is a random vector in a bounded set and finds performance limitations in the average setting.

Chapter 5

Finite Capacity Feedforward Control: Performance Synthesis

In this chapter, we consider a simple network, in which the plant and controller are local to each other, but are together driven by a remote reference signal that is transmitted through a noisy discrete channel with finite capacity. We first construct an infinite-horizon performance metric that illustrates the tradeoffs between sending the remote control system an accurate reference command, and designing a controller such that the remote system matches a given ideal transfer function. The longer one spends coding the input signal before it enters the channel, the more accurate the signal is that drives the remote control system. However, delays in receiving commands at the remote site negatively affect performance. We then simultaneously synthesize the controller and encoder lengths that meet specified model matching objectives in the case where the encoder generates block codes [16], and the plant and ideal model are both first-order SISO systems. In general, synthesis of each cannot be done separately due to the tight interplay between the communication link and control system. Finally, we illustrate performance sensitivity to the poles of the plant and model, and to the channel noise.

5.1 Problem Formulation

We consider the *simple feed-forward network*, shown in Figure 5-1, in which a plant and controller are both remote and separated from the reference command by a discrete communication channel.

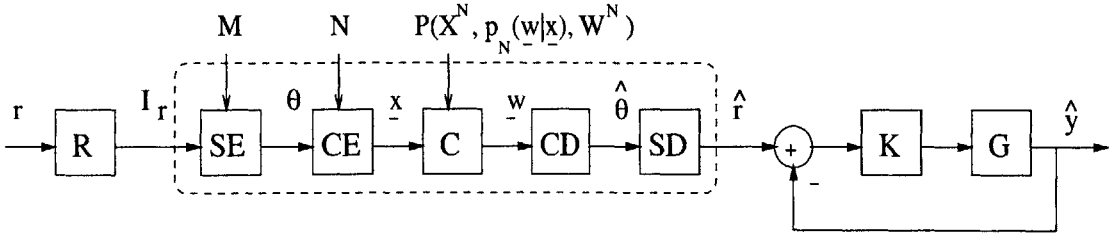

Figure 5-1: Problem Set Up

Specifically,

- $r \in C_r = \{r_1, r_2, ..., r_L\}$ is a given finite set of reference signals that may be transmitted,
- $R : C_r \rightarrow I_r$, where $I_r = \{1, 2, ..., L\}$ is an index set, where index j represents r_j, for $j = 1, 2, ..., L$,
- $SE : \{1, 2, ..., L\} \rightarrow \{0, 1\}^{log_2(M)}$ is a source encoder that compresses information about the input signals ($M \leq L$),
- $CE : \{0, 1\}^{log_2(M)} \rightarrow \{0, 1, ..., k\}^N$ is a block channel encoder [16],
- C: is a discrete memoryless channel with input domain $X^N \in \{0, 1, ..., k\}^N$, range $W^N \in \{0, 1, ..., j\}^N$, and corresponding conditional probability distribution $P_N(\underline{w}|\underline{x})$,
- CD : is a channel decoder that maps $W^N \rightarrow$ $\{0, 1\}^{log_2(M)}$ to minimize the probability of decoding error, $P(\theta \neq \hat{\theta})$,

- $SD : \{0,1\}^{log_2(M)} \rightarrow \mathcal{C}_r$ maps the estimate $\hat{\theta}$ to one of the L reference signals [1],
- K is a causal, discrete-time, SISO controller, and
- G is an unstable causal, discrete-time, SISO plant.

Note that G and C, are fixed, while SE, CE, and K are left for design. Both decoders are functions of the encoding schemes and are fixed once SE and CE are determined.

Before constructing a performance metric, we define two parameters that depend on the source encoding scheme and the set $\mathcal{C}_r$.

1. $\beta_{max}(\mathcal{C}_r) = \max_{i,j \in \{1,2,...,L\}} ||r_j - r_i||_p$, (diameter of $\mathcal{C}_r$)
2. $\beta_{min}(\mathcal{C}_r, SE) = \max_{i \in \{1,2,...,M\}} \max_{(k,j) \in \mathcal{B}(i)} ||r_k - r_j||_p$,

where $\{\mathcal{B}(1), \mathcal{B}(2), ..., \mathcal{B}(M)\}$ is a covering of $\mathcal{C}_r$, defined by SE, that satisfies the following properties:

- $\cup_{i=1}^{M} \mathcal{B}(i) = \mathcal{C}_r$,
- $\mathcal{B}(i) \cap \mathcal{B}(j) = \phi$ for all $i \neq j$, $i, j \in \{1, 2, ..., M\}$.

See Figure 5-2 for an illustration of a covering of $\mathcal{C}_r$, defined by a source encoder, and the corresponding β_{max} and β_{min}.

If the channel is ideal with no noise, then source coding is not necessary, which is equivalent to $M = L$ and $SE = I$. In this case, $\beta_{min} = 0$. If, on the other hand, the source encoder compresses all L signals into 1 "ball" or cover, *i.e.*, M=1, then $\beta_{min} = \beta_{max}$. In general, $\beta_{min}(\mathcal{C}_r, SE)$ is a function that monotonically decreases as M increases, and its shape depends entirely on the source encoder compression algorithm and the set of signals, r_k, for $k = 1, 2, ..., L$. See Figure 5-3 for an example.

Going forward, we suppress β_{min}'s dependence on $\mathcal{C}_r$, and SE and β_{max}'s dependence on $\mathcal{C}_r$, for an easier read.

[1] We assume that the source decoder carries in its memory a bank of all possible reference signals in $\mathcal{C}_r$, and that it activates one of them when it receives $\hat{\theta}$.

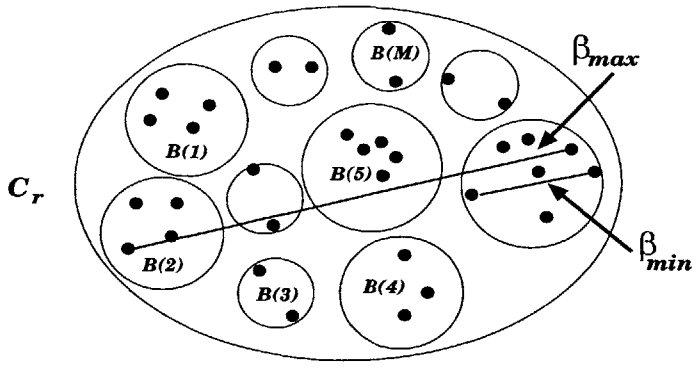

Figure 5-2: Source Encoder Compression and βs

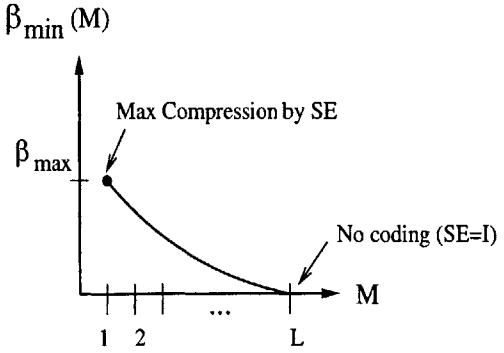

Figure 5-3: β_{min} vs. M

5.1.1 An Equivalent Set Up

In this section, we present a simpler equivalent representation of the detailed set up described above (see Figure 5-4).

In Figure 5-4, we see that the reconstructed command, $\hat{r}$, is just a noisy delayed version of r. However, the noise and the delay are *not* independent of each other. The noise depends on the channel noise, the source resolution M, and the channel block encoding length N, and the delay depends on M and N. Note also that $H = (I + GK)^{-1}GK$.

In this simple set up, we characterize the noise as follows. For a given channel, $\nu \leq \overline{\nu}$, where $\overline{\nu}$ is a random variable that takes on the value β_{max} with probability

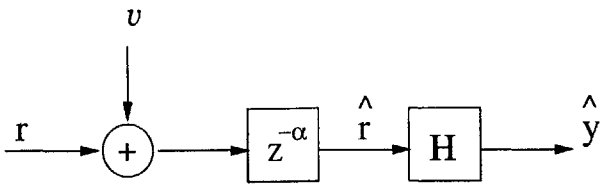

Figure 5-4: Simpler Equivalent Set Up

$P(\theta \neq \hat{\theta})$ and β_{min} with probability $P(\theta = \hat{\theta})$. The delay $\alpha = log_2(M)+N$. We proceed with constructing our performance objective using this simpler representation.

5.1.2 Model Matching Performance Metric

In classical synthesis problems, we may be interested in designing K such that $H = (I + GK)^{-1}GK$ is "close" to some given ideal model transfer function T. That is, we solve the following problem:

$$\begin{aligned} &\min_K ||H - T||_{p-ind} \\ &\text{s.t.} \quad H \text{ is stable.} \end{aligned}$$

Here, we consider the following modified problem that takes into account the communication link in our set up.

$$\begin{aligned} &\min_K \max_{r \in \mathcal{C}_r} E\{||H\hat{r} - Tr||_p\} \qquad (*) \\ &\text{s.t.} \quad H \text{ is stable.} \end{aligned}$$

If we let $\alpha = log_2(M) + N$ and $H_\alpha = z^{-\alpha}H$ (a delayed version of H), we then get that

$$\begin{aligned} d(\hat{y}, y_{ideal}) &\triangleq ||H\hat{r} - Tr||_p \\ &= ||H_\alpha(r + \nu) - Tr||_p \\ &= ||(H_\alpha - T)r + H_\alpha\nu||_p, \end{aligned}$$

where ν is the noise signal. We now take the expectation of the distance function d with respect to the noise upper bound $\overline{\nu}$, and get

$$\begin{aligned} E_{\overline{\nu}}(d) &= P(\theta = \hat{\theta})||(H_\alpha - T)r + H_\alpha \nu_{\overline{\nu}=\beta_{min}}|| + \\ & \quad P(\theta \neq \hat{\theta})||(H_\alpha - T)r + H_\alpha \nu_{\overline{\nu}=\beta_{max}}|| \\ &\leq P(\theta = \hat{\theta})\{||(H_\alpha - T)r|| + ||H_\alpha||\beta_{min}\} + \\ & \quad P(\theta \neq \hat{\theta})\{||(H_\alpha - T)r|| + ||H_\alpha||\beta_{max}\} \\ &\leq ||H_\alpha||\{\beta_{min} + (\beta_{max} - \beta_{min})P(\theta \neq \hat{\theta})\} + \\ & \quad ||(H_\alpha - T)||\overline{r}, \\ & \quad (1) \end{aligned}$$

where $\overline{r} = max_{i=1,\ldots,L}||r_i||_p$.

From Information Theory [16], we recall that an upper bound on the probability of decoding error, $P(\theta \neq \hat{\theta})$, given any discrete memoryless channel is

$$P(\theta \neq \hat{\theta}) \leq (M-1)^\rho \{\tfrac{1}{k} \sum_{l=1}^{j} [\sum_{m=1}^{k} p(l|m)^{\frac{1}{1+\rho}}]^{1+\rho}\}^N$$

$$\triangleq \overline{\omega},$$

where $0 \leq \rho \leq 1$. Going forward, we pick ρ that minimizes this upper bound for our example. It is important to note that the upper bound decays quickly as N increases when the channel has less noise. For example, we compute the bound for the binary symmetric channel (BSC) [16] in Figure 5-5 for different noise levels, where p is the probability of an error.

Finally, we plug in the upper bound, $\overline{\omega}$, into inequality (1) and get

$$E_{\overline{\nu}}(d) \leq ||(H_\alpha - T)|| \cdot \overline{r} + ||H_\alpha||\eta,$$

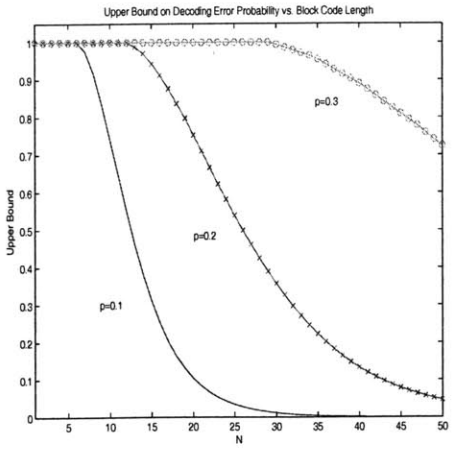

Figure 5-5: Upper Bound on Probability of Decoding Error: BSC

where $\eta \triangleq \{\beta_{min} + (\beta_{max} - \beta_{min})\overline{\omega}\}$.

5.1.3 Tradeoffs Between Communication and Control Objectives

We now make some high-level observations on components of the upper-bound of $E_{\overline{\nu}}(d)$ computed above as the code lengths vary.

- $||(H_\alpha - T)|| \cdot \overline{r}$: increases if N or M increases.
- $||H_\alpha||\eta$: generally increases if M increases, and decreases if N increases.

Overall, if M is fixed and N increases, the estimate of the reference signal improves ($\overline{w}$ decreases [2]), but the delay of the control system receiving $\hat{r}$ increases, which negatively impacts performance. If M increases and N is fixed, the source encoder more accurately represents the input signals (less compression), but the probability of decoding error increases as there are more possible messages that can be sent through

[2]We note that $\overline{w}$ decreases as N increases only if the channel encoder rate, $\frac{log_2(M)}{N}$, is less than the Shannon Capacity of the Channel, C [16]. The channel encoder rate is defined as the number of input symbols entering CE divided by the number of output symbols leaving CE.

the channel. In addition, delay of the control system receiving $\hat{r}$ again increases, which negatively impacts performance. We set out to quantify these tradeoffs.

5.1.4 Problem Statement

In this section, we state questions that we are interested in answering for the above set up. We assume that the reference signals in $\mathcal{C}_r$ lie in l_2, and the output signals lie in l_∞. Thus, the induced norm between the input, $r \in \mathcal{C}_r$, and output, $\hat{y}$, is upper-bounded by the $\mathcal{H}_2$ norm of the network.

We observe that

$$\begin{aligned} E_{\overline{\nu}}(d) &\leq ||(H_\alpha - T)||_{\mathcal{H}_2} \cdot \overline{r} + ||H_\alpha||_{\mathcal{H}_2} \cdot \eta \\ &\leq \sqrt{2}\sqrt{||(H_\alpha - T)||^2_{\mathcal{H}_2} \cdot \overline{r}^2 + ||H_\alpha||^2_{\mathcal{H}_2} \cdot \eta^2} \\ &= \sqrt{2}\, || \begin{bmatrix} (H_\alpha - T)\overline{r} & H_\alpha \eta \end{bmatrix} ||_{\mathcal{H}_2}. \end{aligned}$$

To get the 2nd inequality above, we let $|g_1| \triangleq ||(H_\alpha - T)||_{\mathcal{H}_2} \cdot \overline{r}$, $|g_2| \triangleq ||H_\alpha||_{\mathcal{H}_2} \cdot \eta$, and then use the fact that $|g_1| + |g_2| \leq \sqrt{2}\sqrt{|g_1|^2 + |g_2|^2}$.

Now, instead of solving (*), which, in general, is not easily computable for broad classes of encoders and channels, we seek to minimize the above upper bound by solving the following problem.

$$\begin{aligned} &\min_{K(M,N)} \sqrt{2}\, || \begin{bmatrix} (H_\alpha - T)\overline{r} & H_\alpha \eta \end{bmatrix} ||_{\mathcal{H}_2} \qquad (**) \\ &\text{s.t. } H \text{ is stable.} \end{aligned}$$

Note that if the channel is ideal ($\overline{w} = 0$), then no coding is necessary, which makes $\beta_{min} = 0$, and therefore $\eta = 0$. The above cost function then reduces to the traditional model matching cost function.

Questions of Interest

Given a causal, unstable, DT, SISO plant, G, a causal, stable, DT, SISO ideal model, T, a discrete memoryless channel, C, and a decreasing function $\beta_{min}(M)$,

1. Solve (**) to synthesize a SISO LTI controller, K^o, as a function of (M, N).
2. Plug $K^o(M, N)$ back into the performance metric and find the code lengths, M and N, that minimize the cost function.
3. Describe the sensitivity of the optimal cost to the poles of the plant and ideal model, and to the channel noise.

5.2 First-Order Example

In this section, we consider the special case where:

- $G(z) = \frac{z}{z-a} \quad |a| > 1,$
- $T(z) = \frac{z}{z-\lambda} \quad |\lambda| < 1,$
- C is a binary symmetric channel (BSC), with bit-flip probability p,

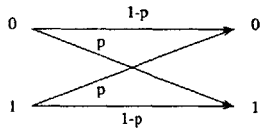

- $\beta_{max} = 1,$
- $\beta_{min}(M) = \begin{cases} 1 & M = 1 \\ \frac{1}{log_2(M)} & M \geq 2. \end{cases}$

5.2.1 Synthesis of Controller

To synthesize the controller as a function of the code lengths, we first parameterize the set of all stabilizing controllers of the remote system $H = (I + GK)^{-1}GK$ [12]. To do so, we first construct one observer-based controller by finding scalars f and l such that $a + af$ and $a + l$ are both stable (have magnitude inside the unit disk). We choose $f = -1$ and $l = -a$. Then, using the method and notation described in [12], we get the following coprime factorization over all stable proper rational functions of the plant, G:

$$N(z) = 1 \quad M(z) = \tfrac{z-a}{z} \quad \tilde{Y}(z) = 1 \quad \tilde{X}(z) = \tfrac{a}{z},$$

where

$$G(z) = \tfrac{N(z)}{M(z)} \quad \& \quad N(z)\tilde{X}(z) + M(z)\tilde{Y}(z) = 1.$$

Then, the set of all stabilizing controllers are of the form $\frac{\tilde{X}(z)+M(z)Q(z)}{\tilde{Y}(z)-N(z)Q(z)}$, for $Q(z)$ being any proper rational stable function. This gives us the following closed-loop transfer function,

$$\begin{aligned} H(z) &= N(z)\tilde{X}(z) + N(z)M(z)Q(z) \\ &= P(z) - U(z)Q(z), \end{aligned}$$

where

$$P(z) \triangleq N(z)\tilde{X}(z), \quad U(z) \triangleq -N(z)M(z).$$

The optimization problem (**), using the parameterization of all stabilizing controllers, is then equivalent to solving

$$\min_{Q(M,N)} \sqrt{2}||\overline{G} - S||_{\mathcal{H}_2},$$

$$\text{s.t.} \quad \{S \in (\overline{u}Q)\overline{V} | Q \text{ is a stable proper rational function}\},$$

where

$$\overline{G} = \left[\begin{array}{cc} \overline{r}(z^{-\alpha}P - T) & \eta z^{-\alpha}P \end{array} \right],$$

$$\overline{u} = z^{-\alpha}U,$$

$$\overline{V} = \left[\begin{array}{cc} \overline{r} & \eta \end{array} \right].$$

Note that we supress the z-dependence on z-transforms for a more compact notation (eg. $U = U(z)$).

Before solving for the optimal S^o, we recall that any stable proper rational function can be written as the product of an all-pass filter and a minimum-phase filter (see [12] for details). We can then factor $\overline{u}$ as follows:

$$\overline{u} = \overline{u}_{ap}\overline{u}_{mp} = \{\tfrac{a-z}{(a-z^{-1})(z^{\alpha+1})}\}\{a - z^{-1}\}.$$

Finally, we define $S^o = \overline{u}Q^o\overline{V}$, and for all stable rational proper functions Q, the following statements hold (in $\mathcal{H}_2$ norm).

$$\begin{aligned} ||\overline{G} - S|| &= ||\overline{G} - \overline{u}Q\overline{V}|| \\ &= ||\overline{G} - \overline{u}_{ap}\overline{u}_{mp}Q\overline{V}|| \\ &= ||\overline{u}_{ap}(\overline{u}_{ap}^{-1}\overline{G} - \overline{u}_{mp}Q\overline{V})|| \\ &= ||\overline{u}_{ap}^{-1}\overline{G} - \overline{u}_{mp}Q\overline{V}|| \\ &= || \ [\overline{u}_{ap}^{-1}\overline{G}]_{\mathcal{H}_2} + [\overline{u}_{ap}^{-1}\overline{G}]_{\mathcal{H}_2^\perp} - \overline{u}_{mp}Q\overline{V}|| \\ &= || \ [\overline{u}_{ap}^{-1}\overline{G}]_{\mathcal{H}_2^\perp} \ || + || \ [\overline{u}_{ap}^{-1}\overline{G}]_{\mathcal{H}_2} - \overline{u}_{mp}Q\overline{V}||. \end{aligned}$$

From the last equality it is easy to see that $\overline{u}_{mp}Q^o\overline{V} = [\overline{u}_{ap}^{-1}\overline{G}]_{\mathcal{H}_2}$. The optimal parameter function is then

$$Q^o = \tfrac{(\overline{u}_{mp})^{-1}}{\overline{V}\overline{V}^*}[\overline{u}_{ap}^{-1}\overline{G}]_{\mathcal{H}_2} \ \overline{V}^*.$$

Recall that $[f]_{\mathcal{H}_2}$ is the projection of a function f onto the $\mathcal{H}_2$ subspace, and g^* denotes the complex-conjugate transpose of a complex-valued vector function g.

Note that $\overline{u}$ and $\overline{V}$ are functions of M and N, therefore, Q^o is also a function of M and N. Finally, the optimal controller, $K^o = \frac{Q^o}{1-GQ^o}$, is a function of M and N. For our first-order example,

$$H^o(M,N) = \frac{C1z}{az-1} + \frac{C2z}{z-\lambda},$$

where

$$C_1 = (a - \tfrac{1}{a})[\tfrac{a\gamma}{k(a\lambda-1)} + 1],$$

$$C_2 = \tfrac{\gamma(\lambda-a)}{k(a\lambda-1)},$$

$$k = \overline{r}^2 + \eta^2,$$

$$\gamma = \lambda^\alpha[\tfrac{(a^2-1)\overline{r}^2}{\lambda-a} + a\overline{r}^2].$$

5.2.2 Synthesis of Code Lengths

Now that we have the optimal closed-loop transfer function as a function of code lengths, we look for the optimal (M^o, N^o) pair that minimizes the cost function $\sqrt{2}||\overline{G} - S||_{\mathcal{H}_2}$, and the corresponding optimal closed-loop transfer function H^o. We set $a = 1.2, \lambda = 0.95, p = 0.01$, and $\overline{r} = 0.2$ and find that the minimum cost is 0.6194 and occurs when $M^o = 32$, and $N^o = 13$. The corresponding optimal control system is

$$H^o = \frac{0.0687z}{1.2z-1} + \frac{0.1693z}{z-0.95}.$$

5.2.3 Performance Sensitivity

In this section, we investigate the sensitivity of the optimal cost to the poles of the plant and model, and to the channel noise.

Figure 5-6 illustrates how the channel code length, N, impacts the optimal cost for different unstable plant poles, when $\lambda = 0.95$ and the bit-flip probabilities of the BSC are 0.01, 0.2, and 0.4. Figure 5-7 illustrates the optimal cost for different levels of channel noise when $\lambda = 0.12$. For these experiments, $\overline{r} = 0.2$, and $M = 1$, while N and a varied.

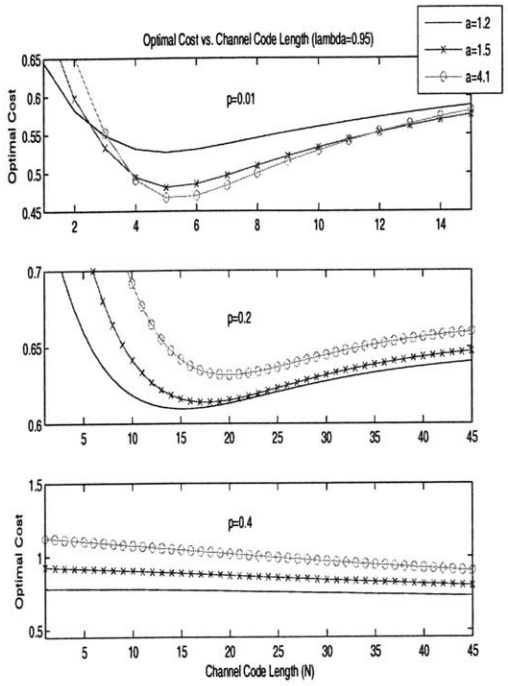

Figure 5-6: Optimal Cost vs. Channel Code Length (N): ($\lambda = 0.95$)

From Figures 5-6 and 5-7, we make the following observations.

- *Sensitivity to plant pole*: The optimal code length increases as the magnitude of the unstable pole increases.

- *Sensitivity to channel noise*: As the channel noise increases, more coding is necessary to reach a minimum cost. However, for very noisy channels, the optimal code length is too long to be of use when implemented as the delay is too large. In such situations, recall that our upper bound on the cost, which was

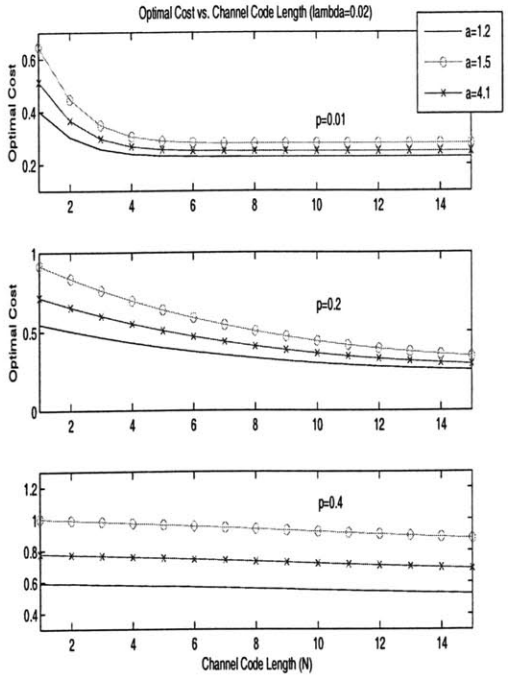

Figure 5-7: Optimal Cost vs. Channel Code Length (N): ($\lambda = 0.02$)

obtained using the upper bound on the probability of decoding error described in section 5.1.2, is not useful.

- *Sensitivity to ideal model pole*: The closer the model pole is to the unit disk, the more coding improves performance. That is, we see the tradeoffs between sending the remote system an accurate reference command and meeting performance.

5.2.4 Ideal Solution

In this section, we look at performance sensitivity of the ideal model matching problem (no channel or coding) by setting $\eta = \alpha = 0$. Figure 5-8 illustrates how the optimal cost behaves as the plant pole becomes more unstable (as a ranges from 1.01 to 4.1) for different ideal model poles ($\lambda = 0.95$ and 0.02). As shown in Figure 5-8, we see that when the ideal model pole is close to the unit disk, the ideal optimal cost

($||H-T||_{\mathcal{H}_2}$) is lowest when $a = 4.1$. This is consistent with what we see in Figure 5-6 for very low channel noise ($p = 0.01$), which shows that the optimal cost for $a = 4.1$ is lowest. However, when the ideal model pole is close to the origin, the ideal optimal cost is lowest when $a = 1.01$, which is also consistent with what we see in Figure 5-7 for very low channel noise.

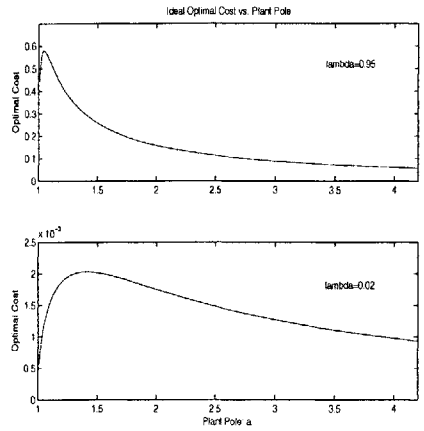

Figure 5-8: Ideal Optimal Cost vs. Plant Pole

5.3 Summary

In this chapter, we simultaneously synthesized the controller and encoder block lengths that meet specified model matching objectives for a first-order plant and model case. We also illustrated performance sensitivity to the poles of the plant and ideal model, and to the channel noise. In short, the tradeoffs between sending an accurate reference command (by implementing some channel coding) and matching an ideal model are most prominent when the channel is not too noisy, the plant pole is more unstable, and when the dynamics of the ideal model are "slow" (ideal model pole is close to the unit disk).

Chapter 6

Future Work

In the future we would like to expand our results for both the simple feedback and feedforward networks, as outlined below.

1. *Simple Feedback Network*

   - (Necessity Condition): In this thesis, we do not derive necessary conditions for finite-gain stability. We discuss why proving necessity is a very difficult problem in section 1.3, and plan to address it in the near future.
   - (Integer Rates): We also do not impose integer constraints on the rates. This adds more technical detail to our framework, which can adapt to integer constraints. This is therefore left for future work.

2. *Simple Feedforward Network*:

   - (Causal Lower Bound): Our lower bounds for the two finite-horizon set ups are obtained for noncausal systems. Deriving a lower bound imposing causality is a more difficult counting problem and we leave it for future work.
   - (Other Communication Channels): We only considered finite-rate noiseless channels in the finite-horizon tracking problems. We would like to extend the results for situations where the channels can be finite-rate noiseless

but with the rate being a random variable. In addition, we would like to explore how finite-capacity discrete memoryless channels impact finite-horizon performance.

Bibliography

[1] Anderson, R.J., Spong, M.W., "Bilateral control of teleoperators with time delay," *IEEE Transactions on Automatic Control*: vol. 34(5), pp. 494-501, May 1989.

[2] Baillieul, J., "Feedback Coding for Information-based Control: Operating Near the Data-Rate Limit," *Proceedings of the 41st IEEE Conference on Decision and Control*, December 2002.

[3] Bertsemis,D., Tsitsiklis, J., "Introduction to Linear Optimization," *Athena Scientific*, 1997.

[4] Delevenne, Jean-Charles, Blondel, Vincent, "Complexity of Control of Finite Automata," *IEEE Transactions on Automatic Control*: preprint.

[5] Bolot, J.C., "End-to-end packet delay and loss behavior in the internet," *SIGCOMM*, September 1993, pp289-298.

[6] Wong, Wing Shing, Brockett, Roger, "Systems with Finite Communication Bandwidth Constraints-I: State Estimation Problems," *IEEE Transactions on Automatic Control*: vol. 42, no. 9, September 1997.

[7] Brockett, Roger W., "Quantized Feedback Stabilization of Linear Systems," *IEEE Transactions on Automatic Control*: vol. 45, pp. 1279-1289, 2000.

[8] Wong, Wing Shing, Brockett, Roger, "Systems with Finite Communication Bandwidth Constraints-II: Stabilization with Limited Information Feedback," *IEEE Transactions on Automatic Control*: vol. 44, no. 5, May 1999.

[9] Dahleh, M.A., Diaz-Bobillo, I., "Control of Uncertain Systems: A Linear Programming Approach," Prentice Hall, 1995.

[10] Delchamps, David, "Stabilizing a Linear System with Quantized State Feedback," *IEEE Transactions on Automatic Control*: vol. 35, no. 8, August 1990.

[11] Delevenne, Jean-Charles, "An optimal quantized feedback strategy for scalar linear systems," *IEEE Transactions on Automatic Control*: accepted in 2005.

[12] Doyle, John, Francis, Bruce, Tannenbaum, Allen "Feedback Control Theory," *Macmillan Publishing Company; New York*, c1992.

[13] Elia, Nicola, Mitter, Sanjoy "Stabilization of Linear Systems With Limited Information," *IEEE Transactions on Automatic Control*: vol. 46, no. 9, September 2001.

[14] Fagnani, Fabio, Zampieri, Sandro, "Stability Analysis and Synthesis for Linear Systems With Quantized Feedback," *IEEE Transactions on Automatic Control*: vol. 48, no. 9, 2003.

[15] Fagnani, Fabio, Zampieri, Sandro, "Quantized Stabilization of Linear Systems: Complexity Versus Performance," *IEEE Transactions on Automatic Control*: vol. 49, no. 9, 2004.

[16] Gallager, Robert, "Information Theory and Reliable Communication," *John Wiley and Sons, Inc.* : New York, 1968.

[17] Ganjefar, Soheil, etal., "Teleoperation Systems Design Using Augmented Wave-Variables and Smith Predictor Method for Reducing Time-Delay Effects," Proceedings of the 2002 IEEE International Symposium on Intelligent Control, October, 2002.

[18] Ishii, Hideaki, Francis, Bruce, "Limited data rate in control systems with networks," *Berlin; New York: Springer*, c2002.

[19] Luck, R., Ray, A., "Experimental verification of a delay compensation algorithm for integrated communication and control systems," *International Journal of Control*, volume 59(6), pp 1357-1372, 1994.

[20] Luck, R., Ray, A., Halevi, Y. "Observability under recurrent loss of data," *AIAA Journal of Guidance, Control and Dynamics*, volume 15, pp 284-287, 1992.

[21] Kitts, C. "Development and Teleoperation of Robotic Vehicles," *AIAA Unmanned Unlimited Systems, Technologies and Operations Conference*, San Diego, California, 2003.

[22] Liberzon, Daniel, "A note on stabilization of linear systems using coding and limited communication," *Proceedings of the 41st IEEE Conference on Decision and Control*, December 2002.

[23] Martins, N.C. and Dahleh, M. A., "Fundamental Limitations of Disturbance Attenuation in the Presence of Finite Capacity Feedback, *American Control Conference* 2005 (Extended version submitted to the IEEE Transactions in Automatic Control).

[24] Martins, N.C., Dahleh M.A., and Elia N.; Stabilization of Uncertain Systems in the Presence of a Stochastic Digital Link, *IEEE CDC*, 2004 (Extended version submitted to the IEEE Transactions in Automatic Control).

[25] Nair, G.N., Evans, R.J., "Stabilization with Data-rate-limited Feedback: tightest attainable bounds," *Systems and Control Letters*, volume 41, 2000, pp. 49-56.

[26] Nair, G.N., Evans, R.J. "Stabilizability of stochastic linear systems with finite feedback data rates", *SIAM Journal on Control and Optimization, Society for Industrial and Applied Mathematics, USA*, vol. 43, no. 2, pp. 413 - 436, July 2, 2004.

[27] Niemeyer, G., "Using Wave Variables in Time Delayed Force Reflecting Teleoperation", *M.I.T. PhD*: 1996.

[28] Sarma, Sridevi, Dahleh, Munther A., Salapaka, Srinivasa, "On Time-Varying Bit-Allocation Maintaining Stability: A Convex Parameterization," *Proceedings of the 43rd IEEE Conference on Decision and Control*, December 2004.

[29] Tatikonda, Sekhar, "Control Under Communication Constraints," *IEEE Transactions on Automatic Control*: vol. 49, no. 7, July 2004.

[30] Tatikonda, Sekhar, Sahai, Anant, Mitter, Sanjoy, "Control of LQG Systems Under Communication Constraints," *Proceedings of the American Control Conference*: pp 2778-2782, June 1999.

[31] Yuksel, Serder, Basar, Tamer, "State Estimation and Control for Linear Systems over Communication Networks," *Proceedings of 2003 IEEE Conference on Control Applications*, Volume 1, June 2003.

[32] Chen, Tongwen, Francis, Bruce, "Optimal Sampled-Data Control Systems," *Springer-Verlag* : Printed in Great Britain, 1996.

[33] Viterbi, Andrew, Omura, Jim "Principles of Digital Communication and Coding," *McGraw-Hill Book Company*: New York, 1979.

[34] P.G. Voulgaris, C. Hadjicostis, R. Touri, "A perfect reconstruction paradigm for digital communications," *Proceedings of the 42nd IEEE Conference on Decision and Control*, Dec. 2003.